

## **DISCLAIMER**

This report was prepared as an account of work sponsored by an agency of the United States Government. Neither the United States Government nor any agency thereof, nor any of their employees, makes any warranty, express or implied, or assumes any legal liability or responsibility for the accuracy, completeness, or usefulness of any information, apparatus, product, or process disclosed, or represents that its use would not infringe privately owned rights. Reference herein to any specific commercial product, process, or service by trade name, trademark, manufacturer, or otherwise does not necessarily constitute or imply its endorsement, recommendation, or favoring by the United States Government or any agency thereof. The views and opinions of authors expressed herein do not necessarily state or reflect those of the United States Government or any agency thereof.

GEIID--036

DE84 015086

## **NOTICE**

**PORTIONS OF THIS REPORT ARE ILLEGIBLE. It  
has been reproduced from the best available  
copy to permit the broadest possible avail-  
ability.**

# **METALLURGICAL EXAMINATION OF, AND RESIN TRANSFER FROM, THREE MILE ISLAND PREFILTER LINERS**

**John W. McConnell, Jr.  
Howard W. Spaletta**

**Published August 1984**

**EG&G Idaho, Inc.  
Idaho Falls, Idaho 83415**

**Prepared for the  
U.S. Department of Energy  
Three Mile Island Operations Office  
Under DOE Contract No. DE-AC07-76IDO1570**

*DISTRIBUTION OF THIS DOCUMENT IS UNLIMITED*

*EB*

**MASTER**

## ABSTRACT

Metallurgical examinations were performed on two EPICOR-II prefilter liners at the Idaho National Engineering Laboratory (INEL) to determine conditions of the liners and identify the minimum expected lifetime of those and other liners stored at INEL. The research work was accomplished by EG&G Idaho, Inc. for the EPICOR-II Research and Disposition Program, which is funded by the U.S. Department of Energy. The EPICOR-II prefilter liners were used to filter radionuclides from contaminated water during cleanup of Three Mile Island Unit 2 (TMI-2). The liners were constructed of carbon steel with a phenolic protective coating and contained organic and inorganic ion-exchange filtration media. Program plans call for interim storage of EPICOR-II prefilters at INEL for up to ten years, before final disposal in high integrity containers at the Hanford, Washington commercial disposal site. This report describes the (a) resin transfer process used to empty liners for examination, (b) removal of metallographic sections from those liners, (c) specimen preparation, and (d) findings from metallographic examination of those specimens. A minimum lifetime for the liners is determined and recommendations are given for storage of wastes from future TMI-2 activities.

## SUMMARY

This report discusses the liner integrity examination of two EPICOR-II prefilter liners that were used during cleanup of Three Mile Island Unit 2 (TMI-2) and presents results of that examination. The work was accomplished by EG&G Idaho, Inc. for the EPICOR-II Research and Disposition Program. Two phenolic coated steel liners, PF-3 (containing organic ion-exchange media) and PF-16 (containing organic ion-exchange media and inorganic zeolite), were selected for metallographic examination. The two liners examined held their resin beds for three years. The intent of the examination was to define internal conditions of liners and ensure that liners could be stored safely at the Idaho National Engineering Laboratory (INEL) for a period of ten years. Results from the examination led to an estimation of the expected lifetime of an EPICOR-II liner.

Fifty EPICOR-II prefilters were transported to INEL between April 1982 and July 1983. Upon receipt, the prefilters either were placed individually in one of two shielded storage silos located in the Hot Shop at Test Area North-Building 600 (TAN-600) or stored in temporary storage casks outside that facility. The ion-exchange media were removed from liners PF-3 and -16 in the Hot Shop using a vacuum transfer system developed at INEL for that purpose and described in this report. Each liner was decontaminated, and a hands-on visual inspection conducted. Metallurgical sections were selected and cut from liner sidewalls using saws.

Metallographic specimens were removed from the sections and mounted, polished, and measured for (a) base metal thickness, (b) thickness of corrosion products, (c) thickness of coating, and (d) surface pits and discontinuities. The specimens were etched and photomicrographs were prepared.

It was determined that the exterior phenolic coatings of both liners were in good condition, although minor handling scrapes and some imperfections acquired during fabrication were observed. The interior

coatings of both liners exhibited blistering and some spalling. Corrosion was evident at each location where the coating had blistered or spalled. In PF-3, an area of coating about 8 x 12 in. had been removed mechanically prior to loading with ion-exchange media to serve as a grounding point for a conductivity probe. That area was encrusted with resin and corrosion products.

Metallographic examination of specimens selected from both liners showed a thin film of corrosion products tightly adhering to the base metal underlying the coating. The effects of corrosion on the base metal were evaluated quantitatively by mechanically measuring the remaining base metal thickness.

The location of greatest buildup of corrosion products was the grounding area for the conductivity probe inside liner PF-3. Metallurgical examination of a section removed from that area revealed no evidence of pitting or pitting-type corrosion. The base metal thickness in that area measured 0.016-in. less than base metal adjacent to the probe. Assuming that a straight-line corrosion rate is applicable and all thinning of the wall was caused by corrosion, it is estimated that EPICOR-II liners will have a lifetime of approximately 50 years.

#### ACKNOWLEDGMENTS

The authors extend thanks to D. Lopez for his work on the design and development of the resin transfer system, J. Stoyack who performed test engineering duties and Hot Cell metallurgical evaluations, and D. Miley for conducting the bulk of the metallurgical examination.

## CONTENTS

ABSTRACT .....	ii
SUMMARY .....	iii
ACKNOWLEDGMENTS .....	v
INTRODUCTION .....	1
BACKGROUND .....	3
Description of EPICOR-II Liner .....	3
Receipt and Storage of Prefilters at INEL .....	3
EXAMINATION METHODS .....	5
RESIN TRANSFER FROM LINERS .....	11
Description of Resin Transfer System .....	11
Tilt Fixture Assembly .....	11
Vacuum Pump and Exhaust Assembly .....	11
Vacuum Head and Wand Assembly .....	13
Water Extraction Assembly .....	13
Resin Transfer Operations .....	14
METALLURGICAL EVALUATIONS .....	16
Visual Examination .....	16
Liner PF-3 .....	16
Liner PF-16 .....	20
Metallographic Examination Observations .....	21
Test Plates .....	21
Liner PF-3 .....	22
Liner PF-16 .....	35
Discussion of Results .....	51
Coating Failure .....	51
Base Metal Surface Condition .....	58
Calculation of Liner Minimum Lifetime .....	59
Evaluation of Base and Weld Metal .....	61
CONCLUSIONS .....	63

ME TALLURGICAL EXAMINATION OF,  
AND RESIN TRANSFER FROM,  
THREE MILE ISLAND PREFILTER LINERS

[NTRODUCTION

The 28 March 1979 accident at TMI-2 released approximately 600,000 gallons of contaminated water to the Auxiliary and Fuel Handling Buildings. That water was decontaminated using a demineralization system called EPICOR-II developed by Epicor, Inc. The contaminated water was cycled through three stages of organic and inorganic ion-exchange media. The first stage of the system was designated the prefilter, and the second and third stages were classified as demineralizers. After the filtration process, the ion-exchange media in a number of prefilters contained radionuclides in concentrations greater than those established for disposal of similar materials as low-level wastes. Fifty prefilters having high concentrations of radionuclides were transported to INEL for interim storage prior to final disposal. A special overpack, or high integrity container, was developed during that storage period for use in disposing of prefilters at the commercial disposal facility in the State of Washington.

During the interim storage period, research has been, and continues to be, conducted on materials from those EPICOR-II prefilters as part of the EPICOR-II Research and Disposition Program funded by the U.S. Department of Energy (DOE). Studies are being conducted on (a) organic ion-exchange resin from selected prefilters and (b) corrosion resistant behavior of the phenolic coated (hereinafter referred to as coating) steel walls of the prefilter liners.<sup>1</sup> The resin will be examined to determine resin degradation, and tests will be performed to obtain characteristics of solidified ion-exchange media. Field tests also will be conducted to study leaching of radionuclides from solidified samples of ion-exchange media placed in several disposal site environments. That research is described in detail in Reference 1. Two liners were examined to determine their integrity and determine if prefilters containing radionuclides can be stored for up to ten years at INEL without failure. [Failure of a liner could result in spread of radioactive waste within the storage system.]

This report discusses the liner integrity examination and presents results of metallographic examination of two liners. Because the construction and coating of EPICOR-II liners are typical of commercial nuclear storage and disposal systems, results of this study might be useful for other applications in the industry. Liners PF-3 and -16 were selected for metallographic examination to define their internal conditions and determine if prefilters could be stored safely at INEL for up to ten years. Those two prefilters had been characterized previously by Battelle Columbus Laboratories (BCL).<sup>2,3</sup> That work included a detailed study of the condition of the ion-exchange media contained within each liner, measurement of radiation dose rates outside and inside the prefilters, and a visual examination of both external and exposed internal metal surfaces of the liners. The ion-exchange media were removed from liners PF-3 and -16 in the TAN-607 Hot Shop using a vacuum transfer system developed at INEL for that purpose and described in this report.

PF-3 and -16 were highly loaded with radionuclides (1900 and 2100 Ci, respectively). It is estimated that radiation doses to the walls and interior coatings of the liners at the time of metallographic sectioning approached  $10^8$  rad.

## BACKGROUND

### Description of EPICOR-II Liner

EPICOR-II liners are 4-ft diameter by 4-ft high cylinders with 1/4-in. thick walls and tops and 1/2 to 5/8-in. thick bottoms (Figure 1). The liners are of welded construction using ASTM Type A-36 carbon steel. The internal and external surfaces are painted with Phenoline<sup>a</sup> 368 coating. A localized area of coating about 8 x 2 in. was removed from the interior surface of each liner. That bare area was used as the grounding point for a conductivity probe for measuring water level in the liner. Each liner contains about 30 ft<sup>3</sup> of ion-exchange media. Liner PF-16 contained both organic ion-exchange resin and inorganic zeolite. Liner PF-3 contained only organic resin. A perforated four-branch influent manifold distributed contaminated water over the exchanger bed, while the effluent was drawn off the liner bottom through a porous multibranched return manifold. Both manifolds are piped to a manifold plate on top of the liner. A vent port and adapters for liquid-level detectors also are located on the manifold plate. A manway is located beside the manifold plate on the liner top. Exchange media were loaded into the liner through the manway. Visual examinations of the liner interiors were conducted through that manway.

### Receipt and Storage of Prefilters at INEL

Each EPICOR-II prefilter was received at the TAN-607 Hot Shop facility of INEL.<sup>4,5</sup> The transportation cask was opened and the prefilter removed remotely and placed in a shielded storage silo. Two silos were designed and fabricated at INEL and erected in the Hot Shop to provide temporary storage and shielding for 48 prefilters. Each silo has a removable shielded cover and is located over a turntable, which is used to position prefilters during storage operations.

---

a. Trade name of the CarboLine Company.

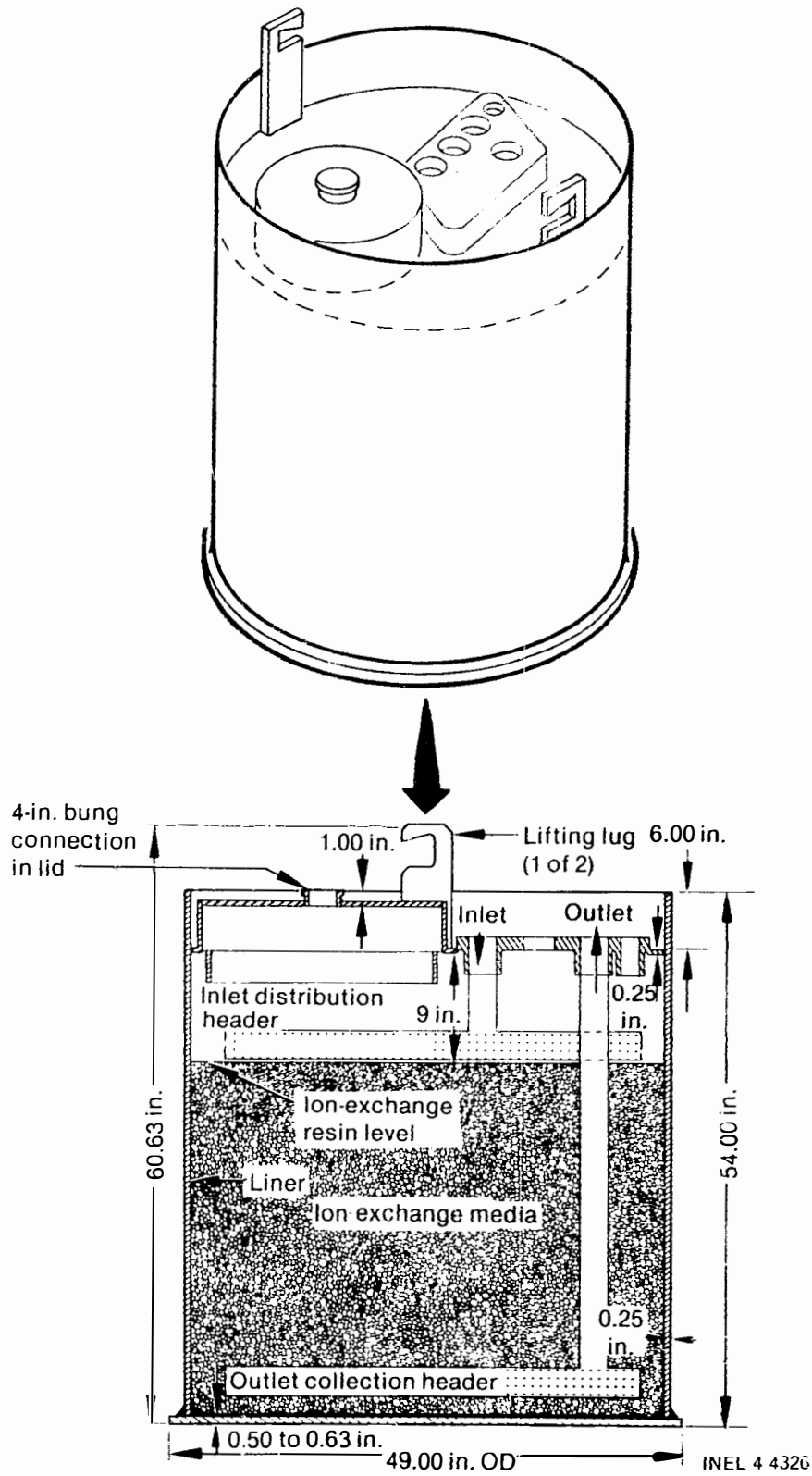


Figure 1. Schematic (isometric and full section) of an EPICOR-II prefilter.

## EXAMINATION METHODS

In preparation for the liner integrity study, the prefilter selected for examination was removed from silo storage and placed in the tilt fixture of the resin transfer system. The ion-exchange media (resins) were transferred, using a vacuum system, to a new replacement liner. The empty liner then was decontaminated and hands-on visual and remote video examinations were conducted. Locations selected for removal of metallurgical sections were marked on the exterior surface of the liner. Photographs were taken of the interior and exterior surfaces of the liner prior to sectioning. The marked locations coincided with specific areas of interest, such as the top surface of the exchange media, corroded areas on the sidewall, and the bottom to sidewall weld joint of the liner. Metallurgical sections were cut from the liner using hand-held power saws. The sections were washed in demineralized water and dried by gently wiping all surfaces, thereby preserving corrosion products. Surface radiation measurements were made to determine the radiation dose rate from each section. Those sections having radiation readings below 1 R/h  $\beta$ - $\gamma$  at contact were transported to the metallography laboratory of the Auxiliary Reactor Area (ARA), where specimens were prepared for detailed examination inside a ventilated hood. Those sections having radiation measurements above 1 R/h  $\beta$ - $\gamma$  at contact were sent to the Hot Cells of Test Reactor Area (TRA), where specimens were prepared for detailed remote examination inside a shielded hot cell.

Locations of metallographic sections (shown in Figures 2 and 3 for liners PF-3 and -16, respectively) were selected from areas that exhibited discontinuities in the internal surface coatings. Three sections were cut from PF-3, and four sections were removed from PF-16. One section from liner PF-3 was removed from the bare area. Sections were obtained from the cylindrical walls of the liners using a 3-in.-diameter metal-cutting hole saw (Figure 4). A section was removed from liner PF-16 at the junction of the cylindrical wall and bottom of the liner, using a portable reciprocating saw (Figure 5). Sections 2 and 3 from PF-3 and Section 2 from PF-16 were removed from the area corresponding to the top surface of

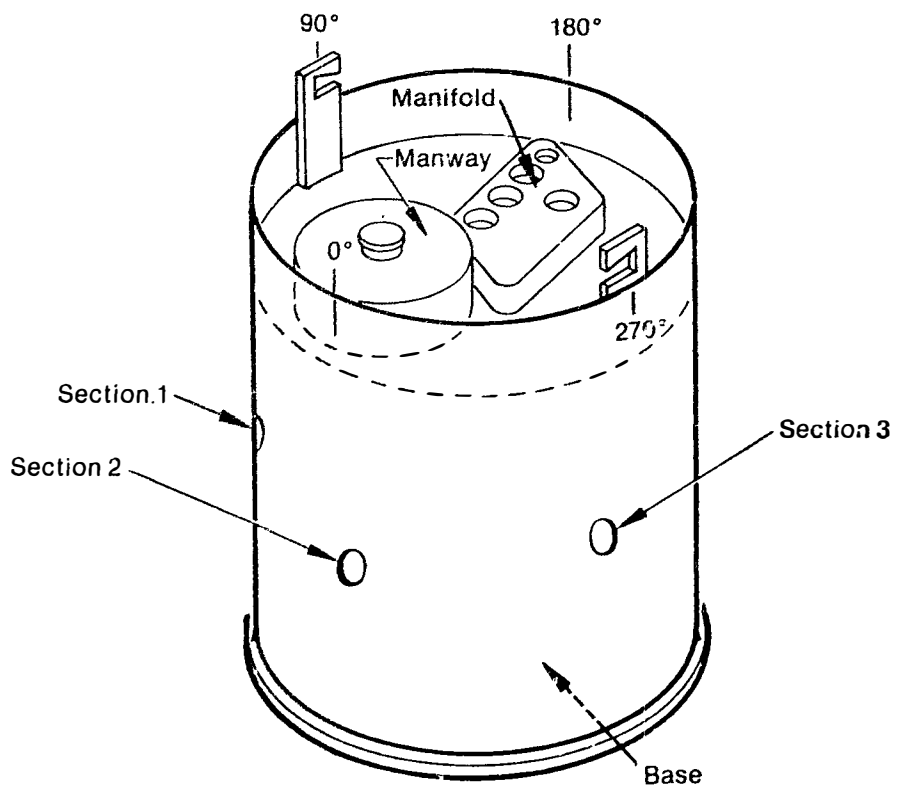


Figure 2. View of liner PF-3 showing locations where metal sections were removed.

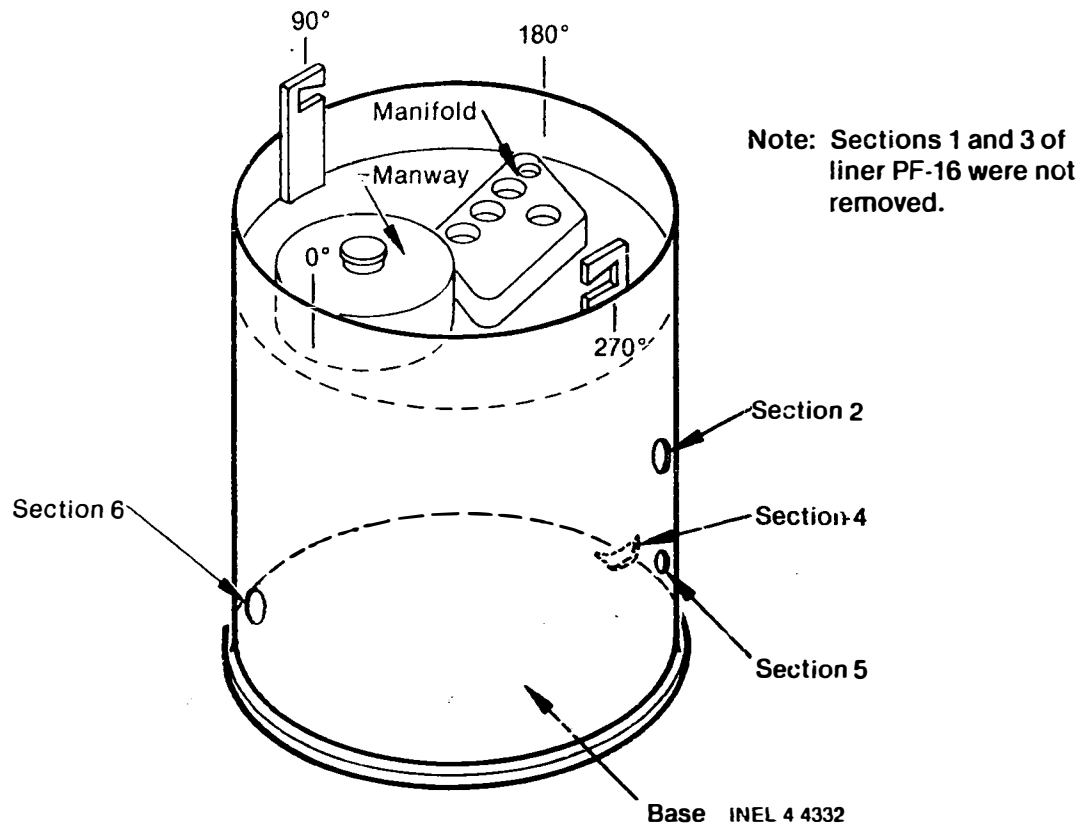


Figure 3. View of liner PF-16 showing locations where metal sections were removed.



INEL 4 4325

Figure 4. Removal of a study section from the cylindrical wall of liner PF-3 using a hole saw.



INEL 4 4327

Figure 5. Removal of a study section from liner PF-16 using a portable reciprocating saw.

the resin bed. The inner surface of Section 1 (from the grounding area for the conductivity probe c liner PF-3) had a  $\beta$ - $\gamma$  radiation reading of 35 R/h at contact, after rinsing and drying, and was submitted to the Hot Cells of TRA for remote examination. All other sections read 1 R/h  $\beta$ - $\gamma$  or less (as shown in Table 1) and were examined in the metallography laboratory of ARA. One specimen from Section 1 of PF-3 was prepared and examined after being decontaminated by mechanically removing most of the corrosion products. Specimens for metallographic examination also were removed from two test plates (identified as Test Plates 1 and 1A) that were coated by Epicor at the same time (and using the same procedures) that the inner surfaces of replacement liners PF-3A and -16A were coated.

TABLE 1. RADIATION MEASUREMENTS OF METALLURGICAL SECTIONS FROM EPICOR-II LINERS PF-3 AND -16

Liner	Section	Location <sup>a,b,c</sup>	Radiation Measurement at Contact, Inside Surface (R/h $\beta$ - $\gamma$ )
PF-3	1	30 in. from bottom, 45° CW from manway	35
	2	30 in. from bottom, below manway	1
	3	30 in. from bottom, 90° CCW from manway	0.6
PF-16	2	30 in. from bottom, 110° CCW from manway	0.250
	4	Junction of bottom and sidewall, 150° CCW from manway	0.020
	5	8 in. from bottom, 120° CCW from manway	0.250
	6	2 in. from bottom, 15° CW from manway	0.030

- a. Locations are approximate and are indicated in Figures 2 and 3.
- b. CW = clockwise, CCW = counterclockwise.
- c. Sections 1 and 3 of PF-16 were not removed from the liner.

Metallographic specimens were obtained and processed as follows:

1. Color photographs were taken of each section before preparing metallographic specimens.
2. Several metallographic cross sections of the liner wall were prepared from those areas of each section that appeared to have a maximum amount of corrosion.
3. Specimens were mounted in plastic, polished, and examined to determine: total base metal thickness, thickness of corrosion products, coating thickness, type of corrosion, and general condition of the base metal. Photomicrographs at 10 and 100 magnifications were prepared for areas of interest.
4. Specimens were etched with Nital reagent (nitric acid and ethyl alcohol) to reveal metallurgical structure, discontinuities, and grain size. Photomicrographs were taken of areas of interest at 100 and 400 magnifications.
5. Corrosion products were identified using electron discharge spectroscopy (EDS).
6. Mounted metallographic specimens were retained in the ARA and TRA Hot Cell archives for future examination, if required.

## RESIN TRANSFER FROM LINERS

The contents of prefilters PF-3 and -16 were transferred, using a resin transfer system, to new replacement liners (identified as PF-3A and -16A). Liners PF-3A and -16A are identical to the other EPICOR-II liners stored at INEL and were purchased from Epicor along with two test plates.

### Description of Resin Transfer System

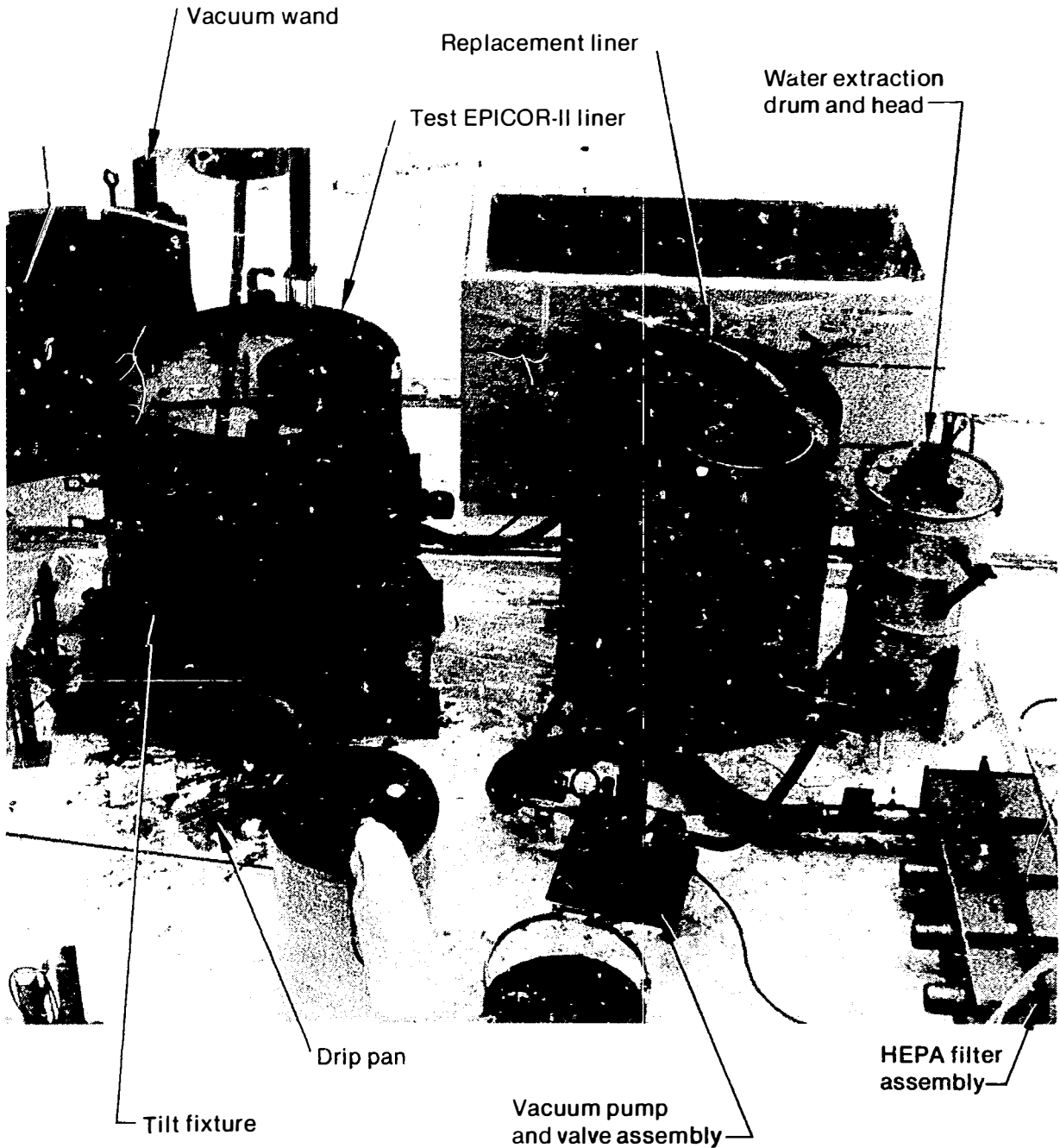
The remotely-operated resin transfer system was installed in the TAN-607 Hot Shop on a drip pan as shown in Figure 6. This system was developed at INEL for the purpose of transferring the difficult to handle layers or mixtures of ion-exchange media (resin) contained in the EPICOR-II prefilters. Those mixtures were composed of zeolite, with cation and anion organic resins, and phenolic, with cation and anion organic resins. The system consists of four assemblies: (a) the tilt fixture, (b) vacuum pump and exhaust, (c) vacuum head and wand, and (d) water extraction-head and drum. The system and its operation are described below.

### Tilt Fixture Assembly

The tilt fixture (left center of Figure 6) supports the liner filled with resin. The fixture with liner is tilted remotely using a cable (pictured at the left of Figure 6) to 15 degrees from vertical. That configuration facilitates removal of resin from the liner. Two jack stands are inserted under the tilt fixture to support it in place during resin transfer operations.

### Vacuum Pump and Exhaust Assembly

The rotary-vane vacuum pump assembly (shown on the drip pan just below the replacement EPICOR-II liner in Figure 6) provides air flow for resin transfer. The pump exhaust is routed to a 4-in.-diameter flexible exhaust hose coupled to a bank of four high-efficiency particulate air (HEPA) filters (lower right of Figure 6). A pressure gauge installed in the exhaust line is used to determine when the filter clogs.



INEL 4 4323

Figure 6. Resin transfer system in the TAN-607 Hot Shop used to transfer resins from one EPICOR-II liner to a replacement liner.

A vacuum gauge and vacuum relief valve are connected to the intake (vacuum) side of the vacuum pump. The intake hose is routed to one port of a four-way manual ball valve. A hose from one of the remaining three ports is routed to the vacuum head on the replacement liner as shown in Figure 6. A hose from a third port of the ball valve is routed to the vacuum head on the 55-gal. water extraction drum shown in Figure 6. The remaining valve port is vented to the atmosphere. The four-way valve supplies vacuum to either the replacement liner (when in the "resin transfer mode") or the water extraction drum (when in the "water extraction mode").

#### Vacuum Head and Wand Assembly

The vacuum wand (a device through which resin is withdrawn from the liner) is a 3/4-in.-diameter stainless steel tube approximately 5-ft long. The outlet end of the tube is connected to a vacuum hose which connects to the liner vacuum head. The outlet end of the wand has an interface grip for the overhead manipulator (C-man). A water-spray nozzle, attached to the inlet end of the wand, sprays water to agitate and suspend resin particles, facilitating their entrance into the wand opening. The nozzle is supplied facility water through a small stainless steel tube and hose. Water flow rate is adjustable to provide the desired effect on the resin particles. The vacuum head (a modified 55-gal. drum closure lid) has connections for the wand hoses, a gage to measure internal vacuum in the replacement liner, and a float-operated vacuum relief valve, which opens when the replacement liner is full.

#### Water Extraction Assembly

The water extraction assembly consists of a vacuum head and modified 55-gal. drum. The drum holds standing water collected from the replacement liner when that liner fills during the resin transfer process. The replacement liner contains a sump strainer connected to the liner effluent port. The water extraction assembly is connected to the replacement liner effluent port by a hose connected to the ball valve on the water extraction

drum head. The water extraction drum head connects to the vacuum pump, contains a gauge for measuring vacuum in the extraction drum, and a float-operated vacuum relief valve identical to the valve on the replacement liner vacuum head. The drum is equipped with a liquid-level sight glass and a water-drain ball valve at the bottom of drum. Waste water is routed from the drain valve to the warm-waste drain of the Hot Shop.

#### Resin Transfer Operations

To begin transfer operations, the liner was placed in the tilt fixture, the manway cover and lockring were removed, the fixture was tilted, and jack stands were placed under the fixture. The O-man positioned the wand in the resin, and the wall-mounted manipulator positioned a TV camera and lights for remote viewing of the operation. Waterflow was initiated to the water-spray nozzle of the wand to agitate the resin, and the vacuum pump was started. When the internal pressure in the replacement liner reached a negative pressure of about 8-in. Hg, the resin was transferred through the wand into the replacement liner. During transfer operations, the vacuum in the replacement liner increased to a steady state of about 15-in. Hg. Transfer of resin continued until the water/resin level in the replacement liner tripped the float valve. The wand spray water was turned off, water extraction ball valve opened remotely, four-way ball valve switched to the "water extraction mode," and replacement liner vented through the open vacuum relief valve. As the vacuum increased in the water extraction drum, water was transferred from the bottom of the replacement liner, through the extraction hose, to the water extraction drum, until the relief valve tripped (which signaled that the drum was full and the vacuum was zero). The ball valve then was opened remotely, and the water in the drum drained into the warm-waste drain of the Hot Shop. The ball valve was closed and the vacuum relief valve of the water extraction head was reset. The procedure was repeated until all standing water was removed from the replacement liner.

After removal of water from the replacement liner, the relief valves of the water extraction head and replacement liner vacuum head were reset remotely. The drain valve of the water extraction drum and the water extraction valve were reset, and the four-way ball valve was set to the "resin transfer mode." The water spray and vacuum pump were turned on and resin transfer resumed. The cycle was repeated until resin was removed from the liner and standing water was removed from the replacement liner. The vacuum head was removed remotely from the replacement liner manway and replaced with a standard drum head and lockring. The replacement liner (containing the dewatered resin) was placed in one of the two silos in the Hot Shop and the silo lid replaced. The tilt fixture was lowered to the level position and the empty liner removed and placed on the Hot Shop floor. Manual removal of the integral outlet header of the empty liner, and subsequent inspection and metallographic section removal, then was accomplished.

## METALLURGICAL EVALUATIONS

This section describes the visual and metallurgical examinations of liners PF-3 and -16 and the examination of two test plates obtained from Epicor.

### Visual Examination

After transferring the resins to replacement liners PF-3A and -16A, the outlet headers of liners PF-3 and -16 were cut into segments with a hand-held reciprocating saw and removed. The exterior and interior surfaces of the liners were examined visually and photographed (Figures 7 and 8). A heavy shield wall was used to reduce radiation exposure to personnel during the examinations. Contact radiation readings ranged between 1 and 2 R/h  $\beta$ - $\gamma$  on the exterior of PF-3 and between 5 and 8 R/h  $\beta$ - $\gamma$  on liner PF-16. Locations for metallurgical sectioning were marked on the exterior surfaces of the liners.

Visual examination of the liners revealed that the exterior and interior base metal surfaces appeared sound [as was previously reported by BCL in References 2 and 3]. It also was noted that the interior coatings were blistered, loose, and in some locations had spalled or chipped. The coating failures appeared more predominant in liner PF-16 than -3 (see Figures 7 and 8). The manway port on liner PF-3 exhibited moderate corrosion while the manway port of PF-16 had extensive coating damage (Figure 9). The interior surface of liner PF-3 was coated with a thin, rust colored film. Both liners had bands of rust on the interior walls at the level corresponding to the top surface of the resin. Detailed descriptions of visual examinations of liners PF-3 and -16 are given below.

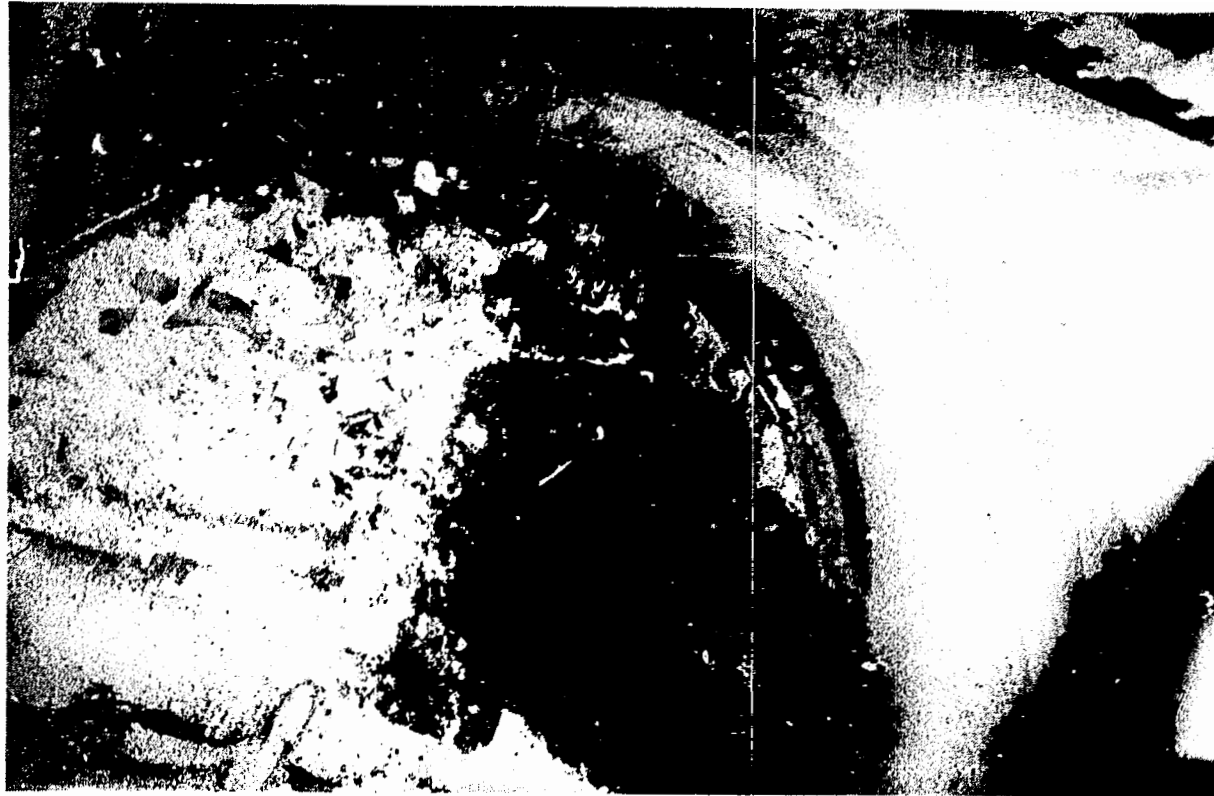
#### Liner PF-3

The exterior surface of liner PF-3 appeared free of flaws. The only visible damage and corrosion appeared to result from routine handling of the liner before examination.



INEL 4 4331

Figure 7. Interior of liner PF-3 showing a dark area covered with rust and resin. The bottom of the liner contains residual resin. Streaks of rust from the manway area and numerous small coating blemishes are visible.



INEL 4 4329

Figure 8. Inside view of liner PF-16 showing broken blisters, flakes of coating, residual resin (dark area), and pieces of BCL coring tool (transparent material).



INEL 4 4330

Figure 9. View of manway port of liner PF-16 showing extensive coating damage.

The interior metal surfaces of the liner appeared free of visible flaws (as previously reported by BCL in Reference 3). The manway port surfaces exhibited moderate corrosion. The interior surfaces of the liner were coated with a thin film of rust. A few penetrations of the coating were observed which were widely dispersed and generally less than 2 in. in diameter. Preferential corrosion was not observed on the side and bottom welds. A thin band of rust was observed inside the liner at the level corresponding to the top surface of the resin.

A dark rectangular area was observed midway up the inner sidewall of liner PF-3. That area was encrusted with resin retained in a matrix of corrosion products (see Figure 7). Discussions between General Public Utilities Nuclear Corporation (GPU Nuclear) and EG&G Idaho (Reference 6) revealed that a localized area of coating had been removed mechanically from each liner using a side-arm grinder. That grinding operation also removed some of the base metal from the liners. The bare area was used as the grounding point for a conductivity probe for measuring water level in the liner. The grounding area in liner PF-3 was estimated from photographs taken during visual examination to be about 8 x 12 in. Resin and corrosion products were observed adhering to that area.

#### Liner PF-16

The exterior sidewall coating of liner PF-16 was free of most visible flaws, with only minor scratches and rust observed. Preferential corrosion was not observed on the vertical side weld. The top and bottom surfaces of the liner showed evidence of scratches and rust in amounts consistent with routine handling of the liner before examination. The bottom to sidewall weld had localized areas of moderate corrosion. The top surface of the liner exhibited areas of moderate to heavy corrosion (predominately around the influent, effluent, and vent ports) and other localized, scattered areas of light to moderate corrosion.

The interior metal surfaces of liner PF-16 appeared free of visible flaws (as previously reported by BCL in Reference 2). The interior surfaces of the manway port exhibited extensive spalling of the coating. A

ring of rust was observed on the sidewall at the level corresponding to the top surface of the resin. Localized areas of moderate corrosion were evident on that ring, with a uniform rust film extending from the ring to the liner bottom. Randomly dispersed coating blisters were evident above and below the rust ring, with some broken blisters observed. A large area where coating had detached (about 3 x 6 in.) was noted near the bottom of the sidewall. Thick corrosion products were observed within the broken blisters and on the large uncoated area. Preferential corrosion was not observed on the bottom to sidewall weld. Small penetrations of the coating were evident on the bottom of the liner, with localized moderate corrosion observed in those areas. The bottom of the liner had a light rust film on the surface of the coating. Manway and remote equipment limitations prevented direct visual inspection of the upper inside surface of the liner wall in PF-16, therefore the bare grounding area for the conductivity probe was not examined.

#### Metallographic Examination Observations

Studies were performed on specimens prepared from the test plates and liners PF-3 and -16. The following discussion presents results of the metallographic examinations.

#### Test Plates

Two test plates were submitted by Epicor to EG&G Idaho for evaluation. Those plates were fabricated by Epicor at the same time (and using the same base metals and coatings) that replacement liners PF-3A and -16A were fabricated. Information obtained from examining the surfaces and coatings of the test plates is compared with data obtained from liners PF-3 and -16. The conditions of the coatings are discussed in this report as are the surface conditions of the base metal of the test plates, which are compared with those conditions observed in liners PF-3 and -16. The test plates provide examples of base metals and coatings that were processed in a controlled manner to process specifications of Epicor. Metallographic specimens were prepared from test plates. The specimens were prepared normal to the coated surfaces and examined at 100 and 400 magnifications.

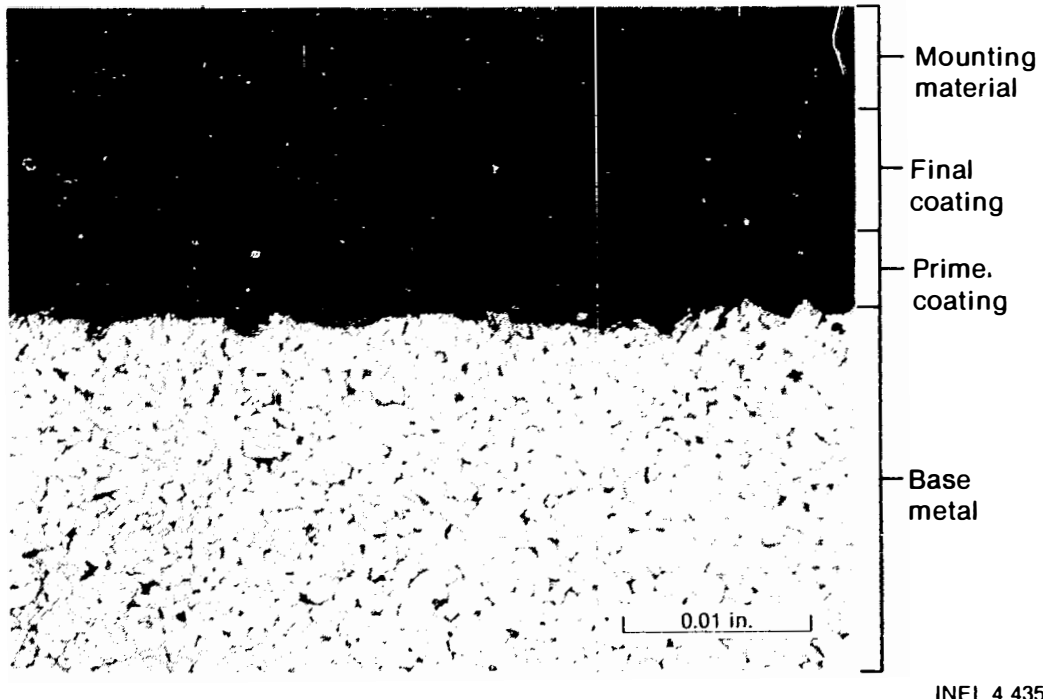
Test Plate 1. Figure 10 shows a fine-grained (ASTM grain size No. 8 or smaller), normal base metal structure representative of the material of Test Plate 1. The base metal had been roughened (probably grit blasted) to about a 500 RMS finish prior to application of the prime coating. The thickness of the prime coating is about 0.005 in. Some porosity in the prime coating is evident. The final coating is about 0.006-in. thick. Considerable porosity appears in the final coating. The total coating thickness is about 0.011 in.

Test Plate 1A. Figure 11 shows a fine-grained (ASTM grain size No. 8 or smaller), normal base metal structure representative of the material of Test Plate 1A. The base metal had been roughened (probably grit blasted) to about a 500 RMS finish before application of the prime coating. The thickness of the prime coating is about 0.008 in. The final coating is about 0.004-in. thick. Some porosity appears in both the prime and final coatings. The total coating thickness is about 0.012 in.

#### Liner PF-3

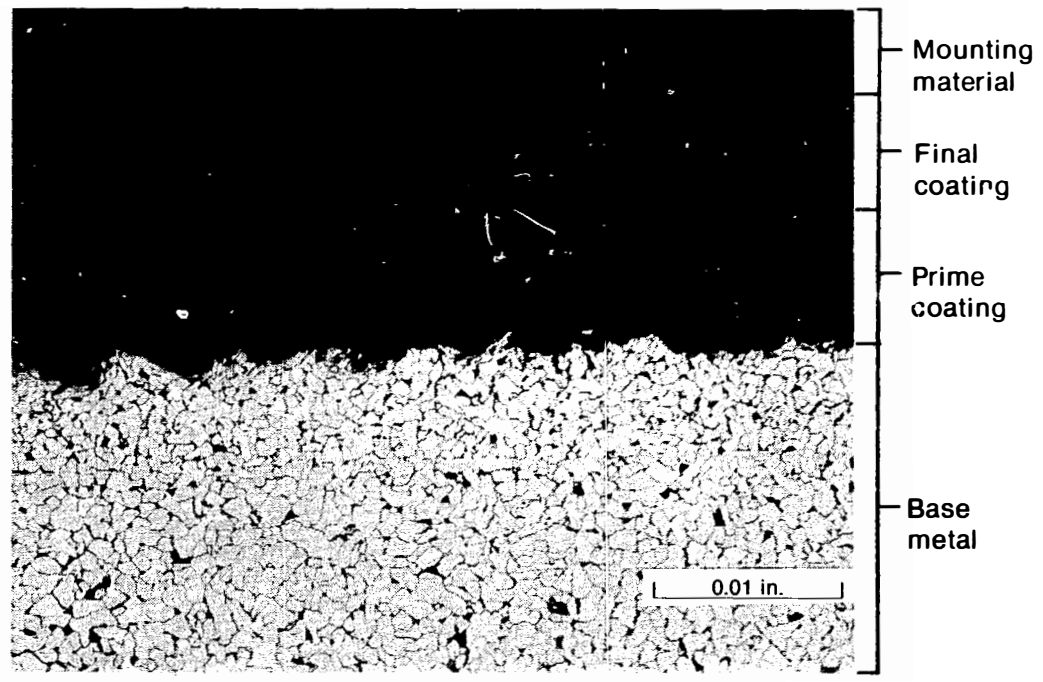
Section 1. Section 1 was removed from the center of the grounding area for the conductivity probe, about 30 in. from the bottom of liner PF-3, 45-degrees clockwise from the manway (see Figure 2). The internal coating had been removed mechanically from that area of the liner. After decontamination by rinsing with mineralized water, contact readings of 35 R/h  $\beta$ - $\gamma$  were measured. Visual examination of the interior surface of the section revealed a heavy deposit of corrosion products and residual resin (Figure 12). The high radiation readings required remote examination of this section in the TRA Hot Cells. Some corrosion products were lost while remotely preparing specimens from Section 1.

Section 1, Specimen 1-B--Figure 13 is a typical photomicrograph normal to the uniformly corroded interior surface observed for Specimen 1-B. No evidence of pitting or pitting-type corrosion was evident. A normal fine-grained (ASTM grain size No. 8 or finer) structure was observed in the base metal (Figure 14). No interior coating was



INEL 4 4358

Figure 10. Photomicrograph normal to the coated surface of Test Plate 1.



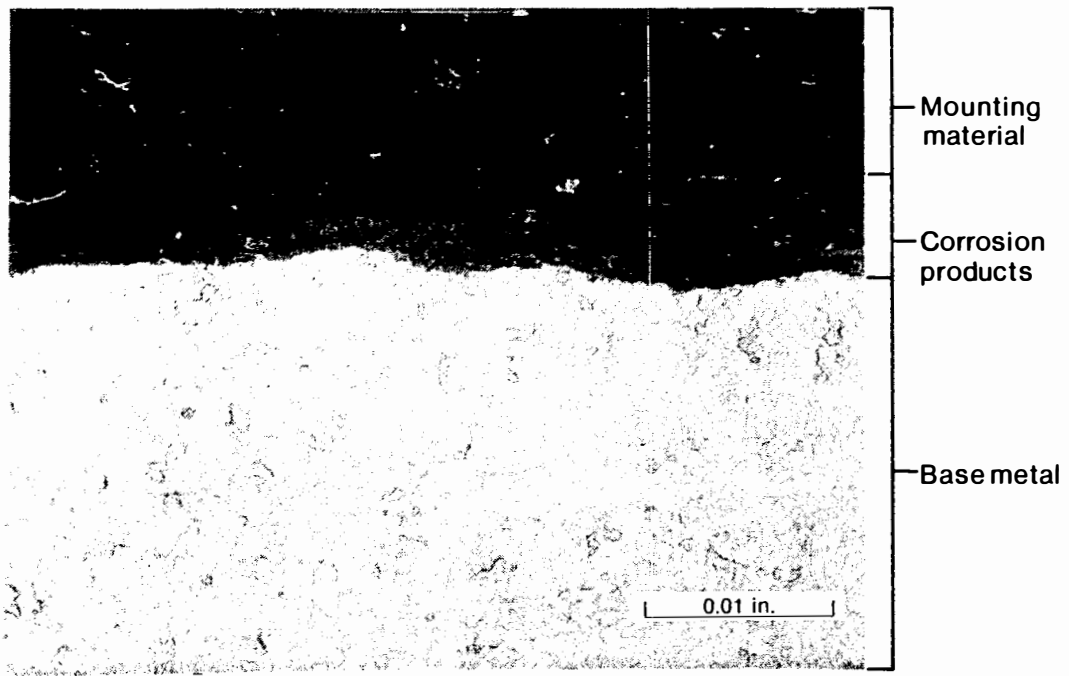
INEL 4 4356

Figure 11. Photomicrograph normal to the coated surface of Test Plate 1A.



INEL 4 4421

Figure 12. Photograph of the interior surface of Section 1 from liner PF-3 showing a heavy deposit of corrosion products and residual resin.



INEL 4 4348

Figure 13. Photomicrograph normal to the interior surface of Section 1 from liner PF-3 showing the uniformly corroded surface.

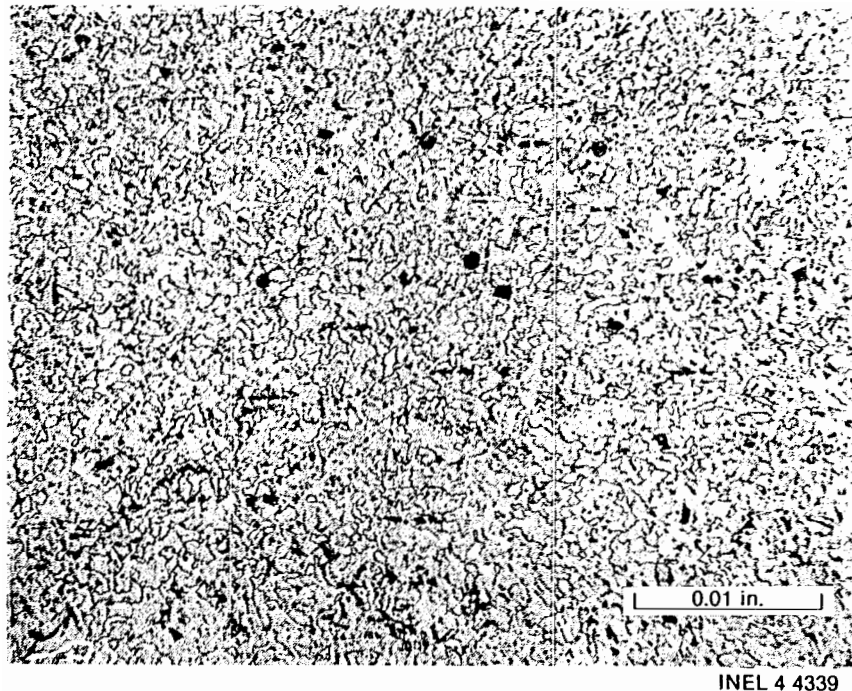


Figure 14. Photomicrograph of Section 1 from liner PF-3 showing a normal fine-grained (ASTM No. 8 or finer) base metal.

evident on the specimen, but the exterior coating was determined to be about 0.010-in. thick. The corrosion products partially spalled off during preparation of the specimen, therefore accurate thickness measurements of corrosion products could not be made.

Section 3. Section 3 was removed from the sidewall of liner PF-3, 90-degrees counterclockwise from the manway, about 30-in. above the bottom of the liner (see Figure 2). That elevation corresponded to the top surface of the resin. Visual examination of the interior surface of Section 3 revealed numerous coating blisters and areas where coating was not adhering to the base metal and had spalled (Figure 15). Light corrosion products under an adherent coating and heavily corroded areas under blisters were observed (Figure 16). The adherent coating is about 0.005-in. thick.

Section 3, Specimen 1-B--The exterior surface of this specimen was examined at 100 magnification (Figure 17), and a heavy exterior phenolic coating of at least three layers was observed. Examination of the exterior surface at higher magnifications revealed corrosion products (about 0.0005-in. thick) between the coating and base metal, with a total coating thickness of about 0.010-in. (Figure 18). Evidence that the coating had been applied over previously present corrosion products is indicated by layers of coating between the base metal and corrosion products (Figure 19).

Comparison of Section 1 (Specimens 1-B and 1-C) with Section 3 (Specimens 3-B and 3-C). Base metal thicknesses of corroded specimens prepared from Section 1 of liner PF-3 (Specimens 1-B and 1-C) were compared with base metal thicknesses of uncorroded specimens taken from the coated area of Section 3 (Specimens 3-B and 3-C). The adherent coating on the surface of specimens from Section 3 protected those specimens from corrosion. Ten thickness measurements were taken of the base metal of Specimen 3-B from Section 3. Those measurements ranged from 0.2493 to 0.2506 in., with an average calculated thickness of 0.2501 in. Those measurements are compared with thickness measurements of a corroded

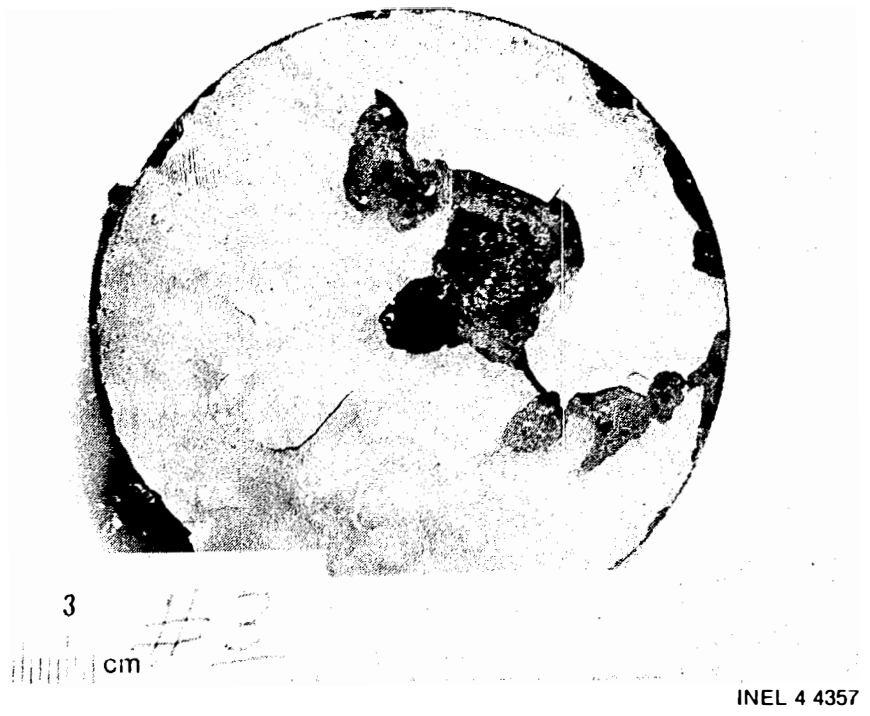
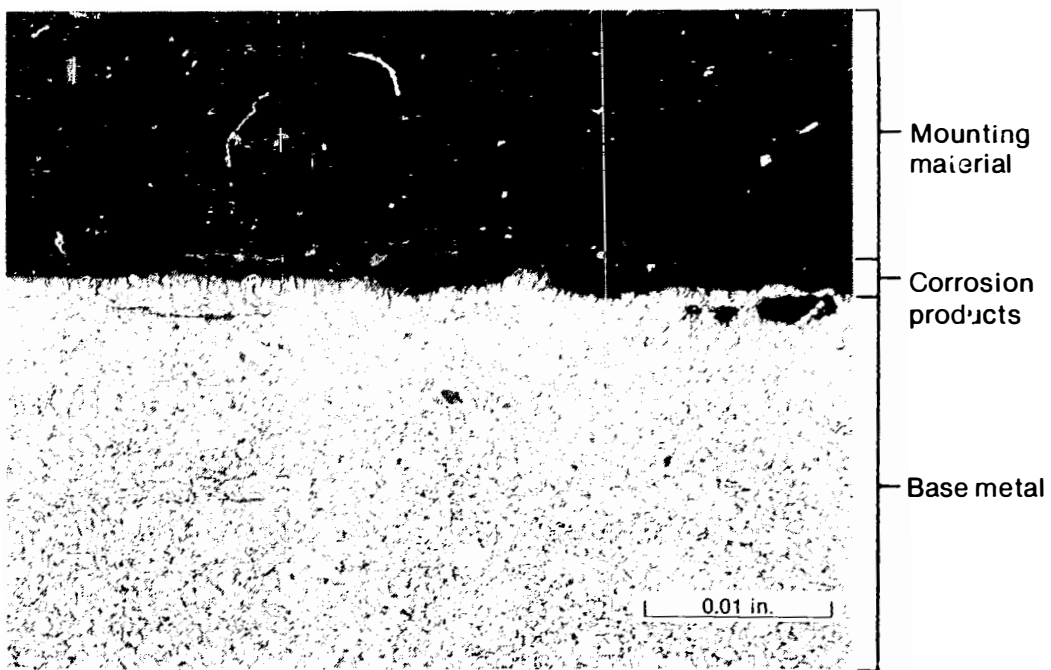
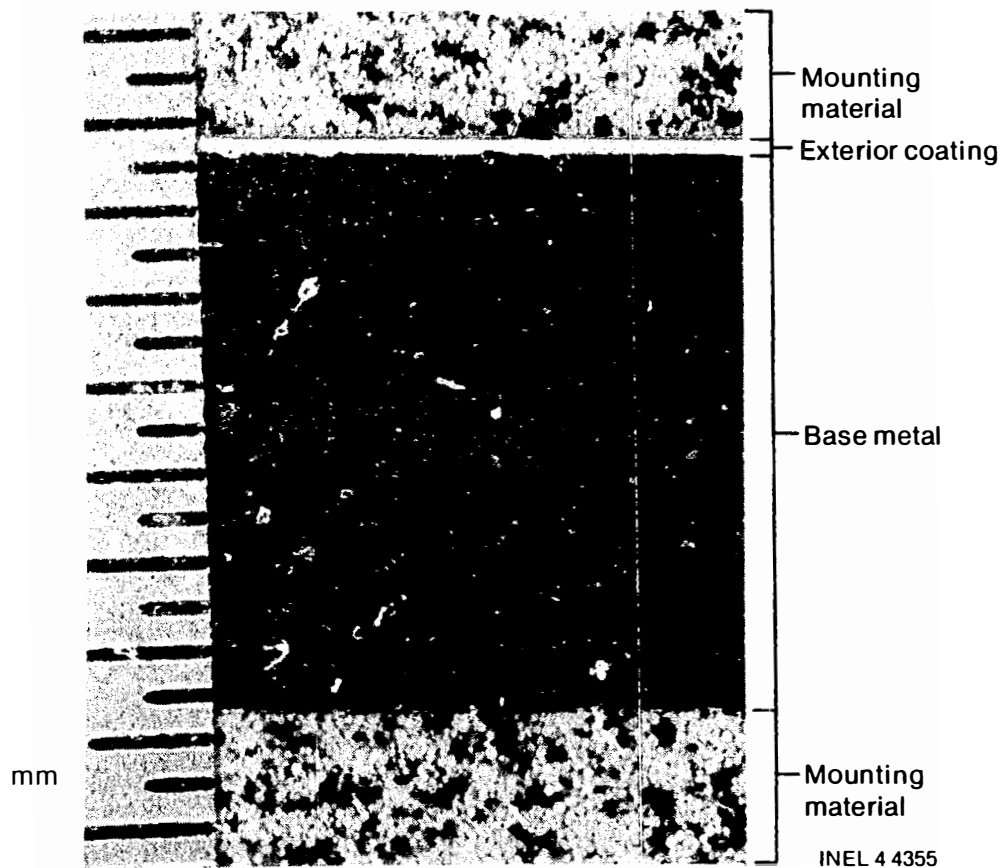


Figure 15. Photograph of the interior surface of Section 3 from liner PF-3 showing coating blisters and areas where coating is missing.



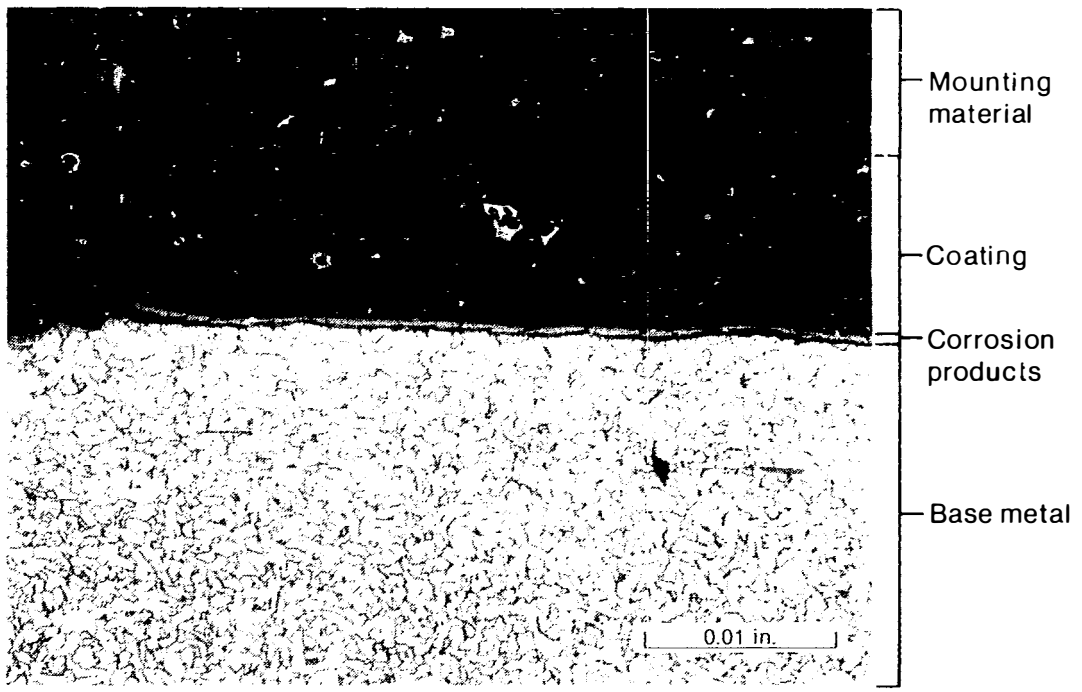
INEL 4 4352

Figure 16. Photomicrograph normal to the interior surface of Section 3 from liner PF-3 showing corrosion products in an area where coating had spalled.



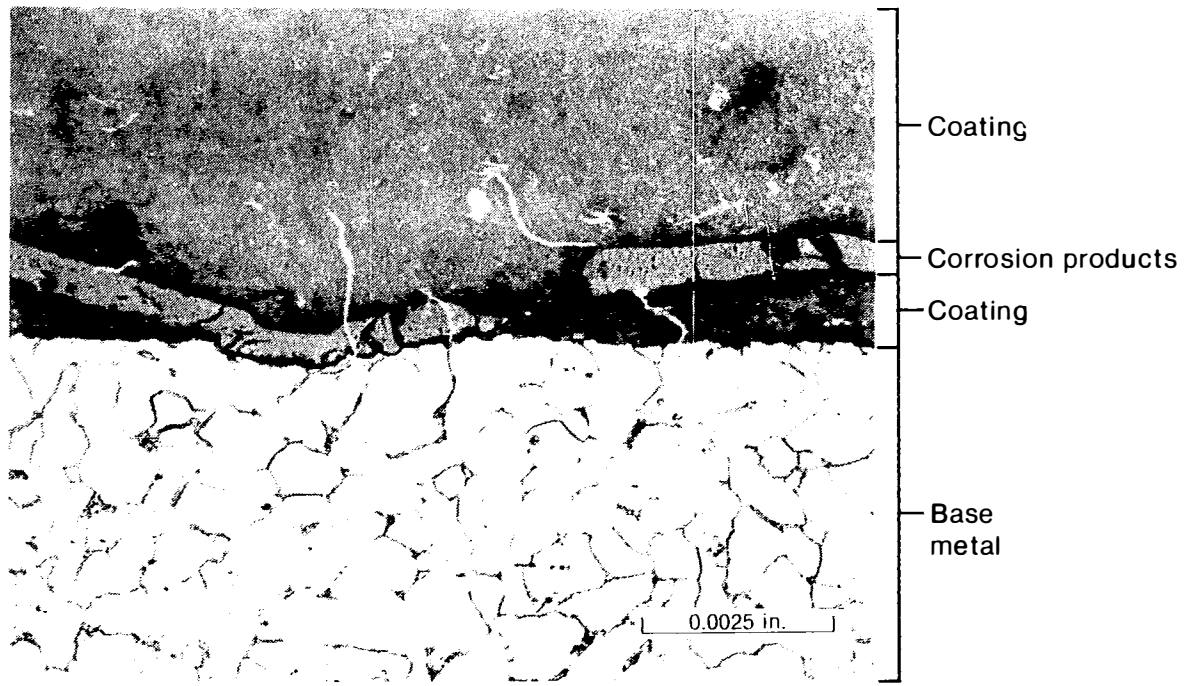
INEL 4 4355

Figure 17. Photomicrograph normal to the wall of Section 3 from liner PF-3 showing the exterior coating and lack of coating on the interior surface.



INEL 4 4354

Figure 18. Photomicrograph normal to the exterior surface of Section 3 of liner PF-3 showing corrosion products between the base metal and coating.



INEL 4 4334

Figure 19. Photomicrograph normal to the exterior surface of Section 3 of liner PF-3 showing coating between the base metal and corrosion products.

specimen (Specimen 1-B) taken from Section 1 (Table 2). Measurements of Specimen 1-B ranged from 0.2346 to 0.2507 in., with an average calculated thickness of 0.2440 in. Thickness measurements of the base metal were obtained for a second coated, uncorroded specimen (Specimen 3-C) from Section 3. Those measurements ranged from 0.2451 to 0.2509 in., with an average base metal thickness of 0.2488 in. (Table 2). A second corroded specimen (Specimen 1-C) taken from Section 1 had base metal thickness measurements ranging from 0.2397 to 0.2496 in., with an average thickness of 0.2456 in. A nominal uncorroded wall thickness of 0.250 in. was calculated from the data.

Visual examination of interior surfaces of specimens prepared from Section 1 revealed a horizontal groove-like indentation on the surface of the grounding area for the conductivity probe. The indentation on Specimen 1-B can be seen in Figure 20. The difference between the thickness of the base metal in the corroded and uncorroded areas can be attributed to (a) corrosion and (b) removal of some base metal while mechanically removing the coating for the conductivity probe.

Section 2. Section 2 was removed from the sidewall of liner PF-3, directly under the manway, about 30-in. above the bottom of the liner, at the level of the top surface of the resin (see Figure 2). Visual examination of the interior surface of Section 2 revealed numerous coating blisters and areas where coating was not adhering to the base metal and had spalled (Figure 21). Corrosion products were evident between the coating blisters and base metal.

Section 2, Specimen 1--Several discontinuities (also referred to as gouges or dings) were observed on the surface of the base metal of Specimen 1 (Figures 22 and 23). A thin film of corrosion products (estimated at 0.0005-in. thick) can be observed between the coating and the base metal. Except for the discontinuities, the metal surface is smooth. Examination of one discontinuity at 400 magnification revealed coating

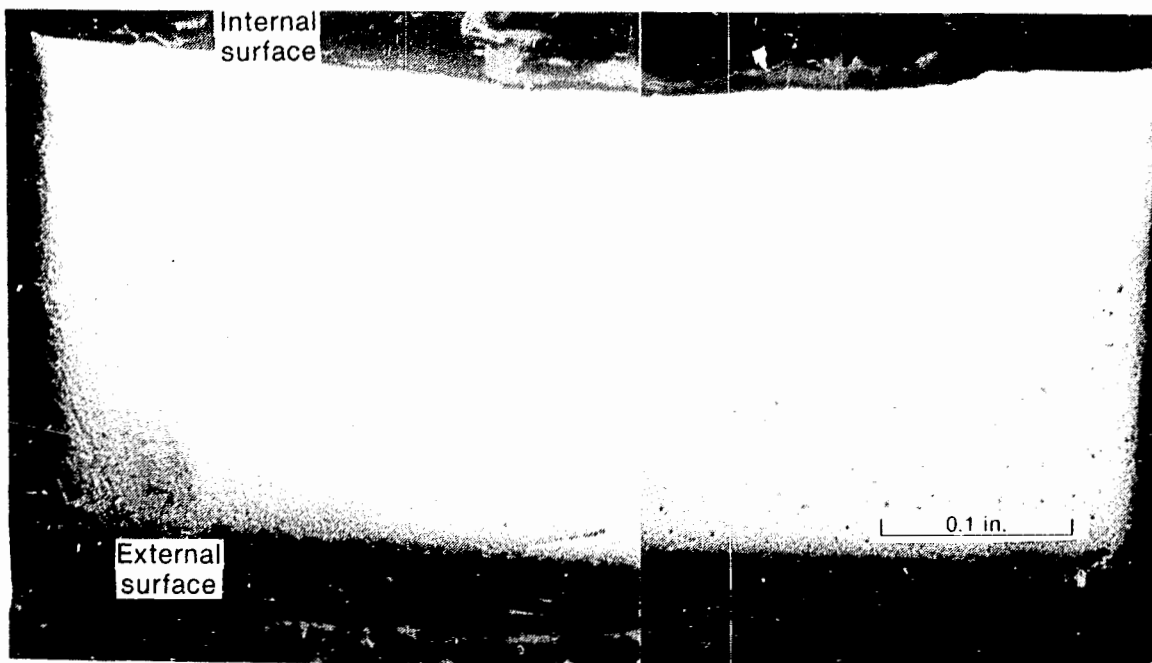
TABLE 2. COMPARISON OF EPICOR-II LINER METAL THICKNESS

<u>Measurement</u>	<u>Metal Thickness of Liner Specimen (in.)</u>			
	<u>1-B (corroded)</u>	<u>3-B (uncorroded)</u>	<u>1-C (corroded)</u>	<u>3-C (uncorroded)</u>
1	0.2503	0.2506	0.2453	0.2451
2	0.2505	0.2505	0.2442	0.2496
3	0.2440	0.2493	0.2494	0.2492
4	0.2378	0.2499	0.2397	0.2467
5	0.2382	0.2501	0.2463	0.2509
6	0.2346	0.2503	0.2467	0.2501
7	0.2354	0.2498	0.2489	0.2483
8	0.2489	0.2500	0.2413	0.2487
9	0.2507	0.2504	0.2451	0.2498
10	0.2494	0.2496	0.2496	0.2496
Average	0.2440	0.2501	0.2456	0.2488
Minimum	0.2346	0.2493	0.2397	0.2451
Maximum	0.2507	0.2506	0.2496	0.2509

adhering to both the base metal and corrosion products, which indicates the surface had been gouged before application of the coating (Figure 24).

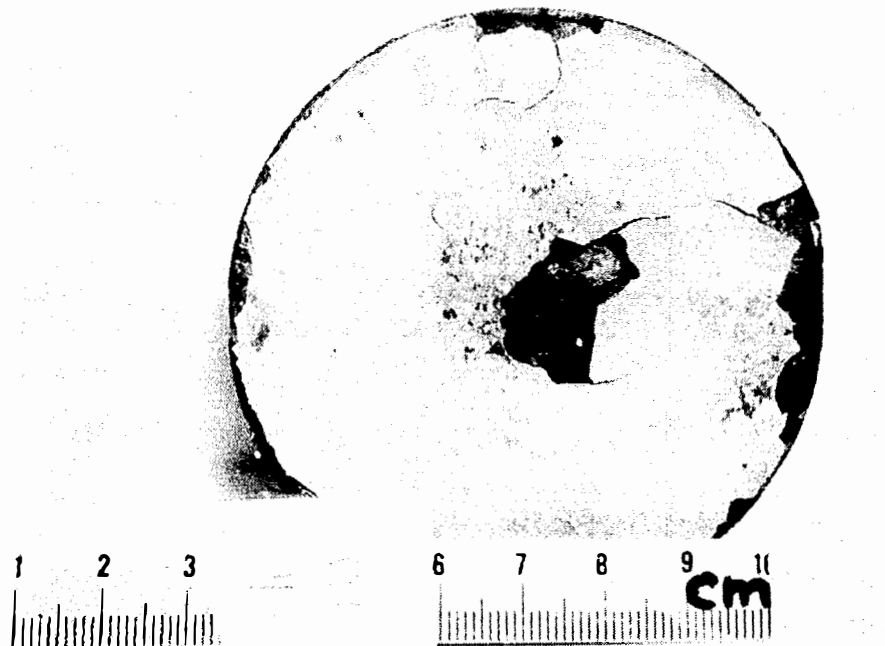
Total coating thickness was measured at between 0.006 and 0.009 in.

Section 2, Specimen 2--Examination of Specimen 2 at  
400 magnification revealed localized areas with intermittent corrosion products between the coating and base metal (Figure 25). That suggests that corrosion in the areas away from blisters in the coating occurred before painting of liners. Examination of Specimen 2 through a coating



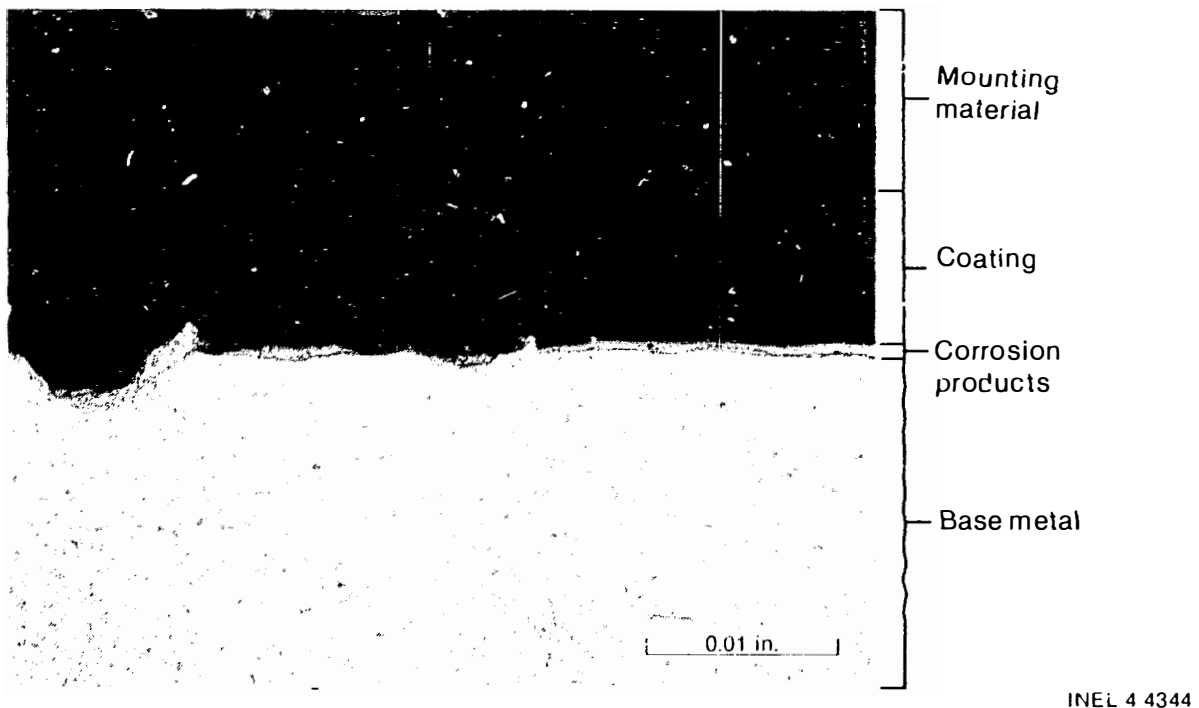
INEL 4 4370

Figure 20. Photomicrograph of Section 1, Specimen 1B (a vertical section from liner PF-3 normal to the grounding area for the conductivity probe) showing the horizontal depression on the internal surface.



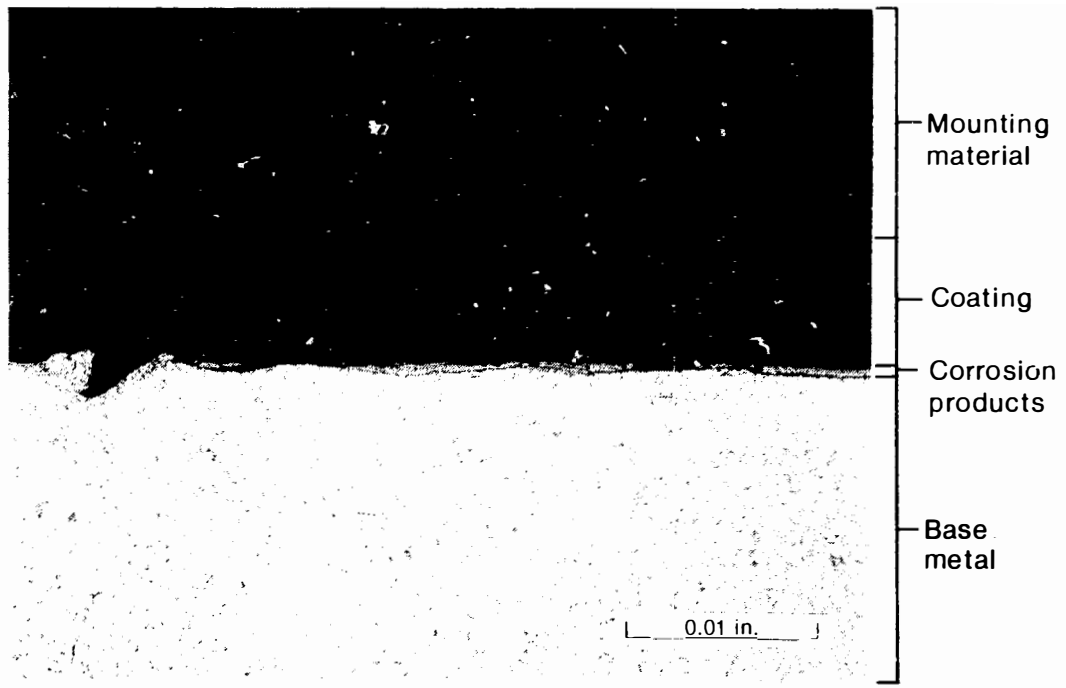
INEL 4 4338

Figure 21. Photograph of the interior surface of Section 2 from liner PF-3 showing coating blisters and areas where the coating is loose.



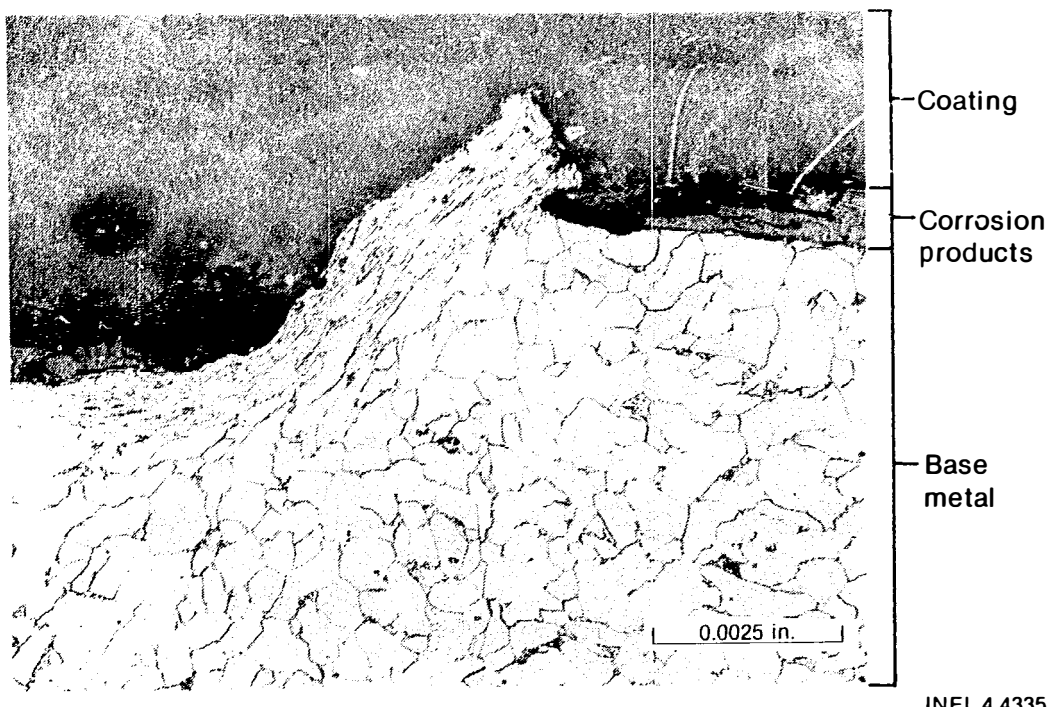
INEL 4 4344

Figure 22. Photomicrograph normal to the interior surface of Section 2 from liner PF-3 showing a surface discontinuity in the base metal.



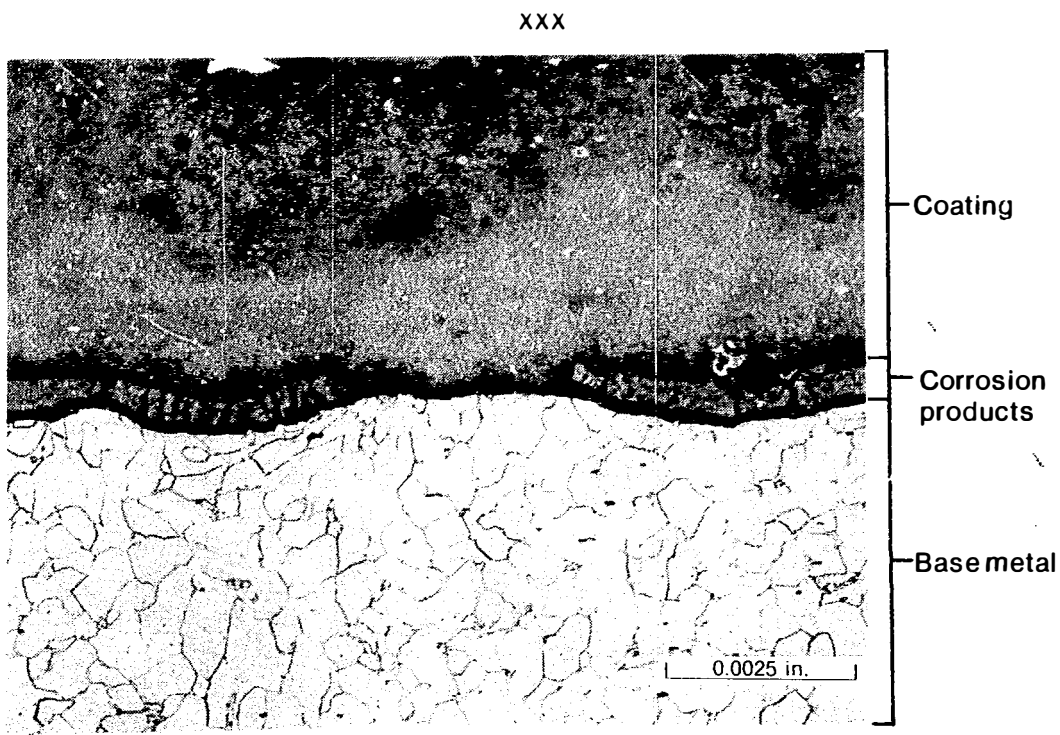
INEL 4 4345

Figure 23. Photomicrograph normal to the interior surface of Section 2 from liner PF-3 showing surface discontinuity in the base metal and an area where the coating is adhering to the base metal with no corrosion products.



INEL 4 4335

Figure 24. Photomicrograph showing greater detail of discontinuity identified in Figure 22.



INEL 4 4336

Figure 25. Photomicrograph normal to the interior surface of Section 2 from liner PF-3 showing corrosion products adhering to the base metal and coating and an area where the coating is adhering to the base metal.

blister revealed corrosion products about 0.004-in. thick between the coating and base metal (Figure 26). Examination of another area of Specimen 2 showed corrosion products adhering to the base metal and not the coating (Figure 27).

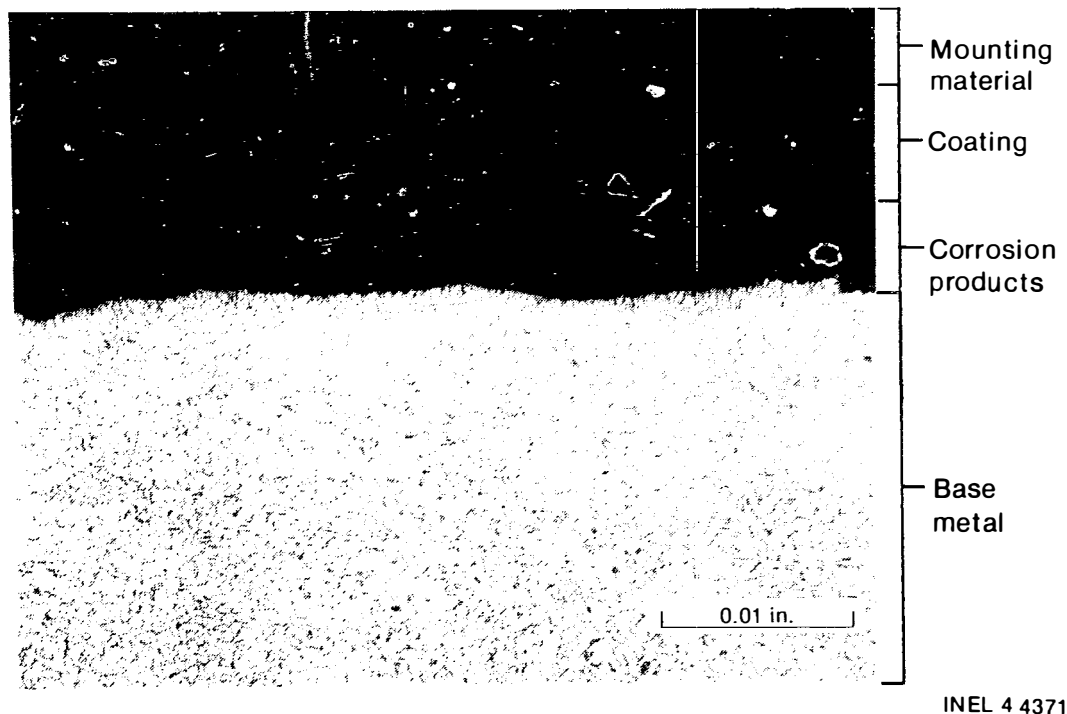
Examination of the exterior surface of Specimen 2 also revealed corrosion products between the coating and base metal. The coating thickness was measured at between 0.009 and 0.012 in.

#### Liner PF-16

Section 2. Section 2 was removed from the sidewall of liner PF-16, about 110-degrees counterclockwise from the manway, about 30-in. above the bottom, at the level of the top of the resin (see Figure 3). Visual examination of the interior surface of Section 2 revealed a nearly defect free surface with one large blister in the coating along one edge of the Section (Figure 28).

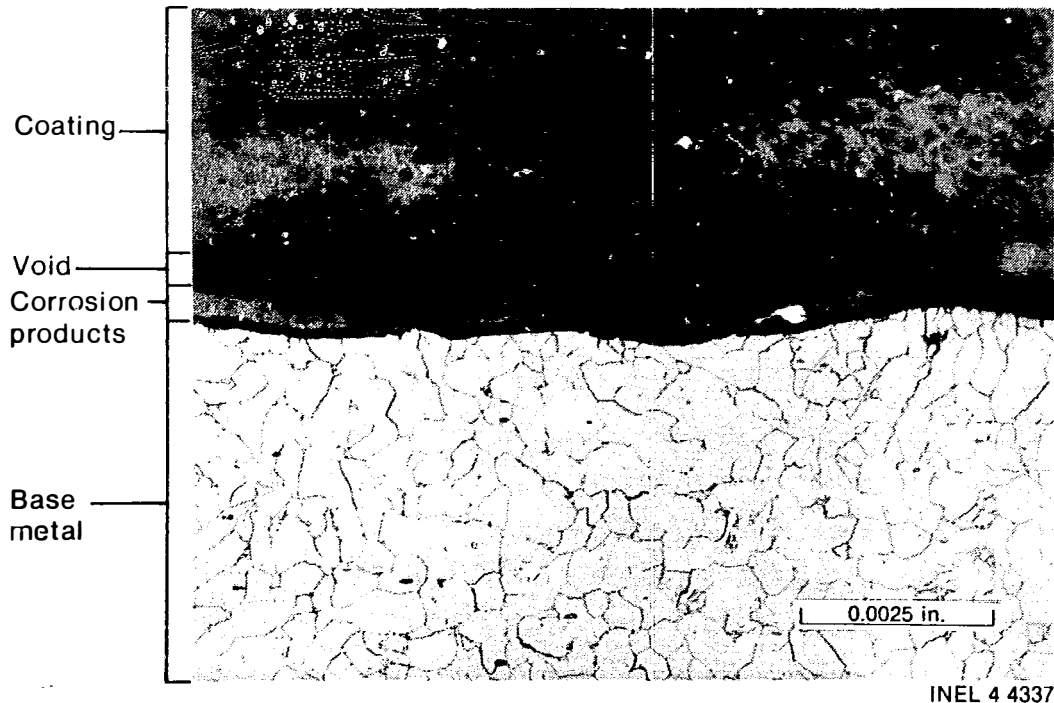
Section 2, Specimen 1--Examination of Specimen 1 revealed some corrosion products (about 0.001 to 0.002-in. thick) between the coating and base metal (Figure 29). Total coating thickness was measured at about 0.012 in. The coating generally adheres to the corrosion products, indicating that corrosion occurred before painting of the liner.

Section 4. Section 4 was removed from the junction of the sidewall and bottom of liner PF-16, about 150-degrees counterclockwise from the manway (see Figure 3). Visual examination of the interior surface of Section 4 revealed numerous blisters in the coating on both the interior surface of the bottom plate and cylindrical wall of the liner (Figure 30). Metallographic specimens were prepared from this section at the locations shown in Figure 31. Figure 31 shows the lack of adherence of the coating to both the internal wall of the liner and surfaces of the welds joining the sidewall to bottom plate. Those welds were made in single passes, joint preparations were not machined prior to welding, and there is a gap



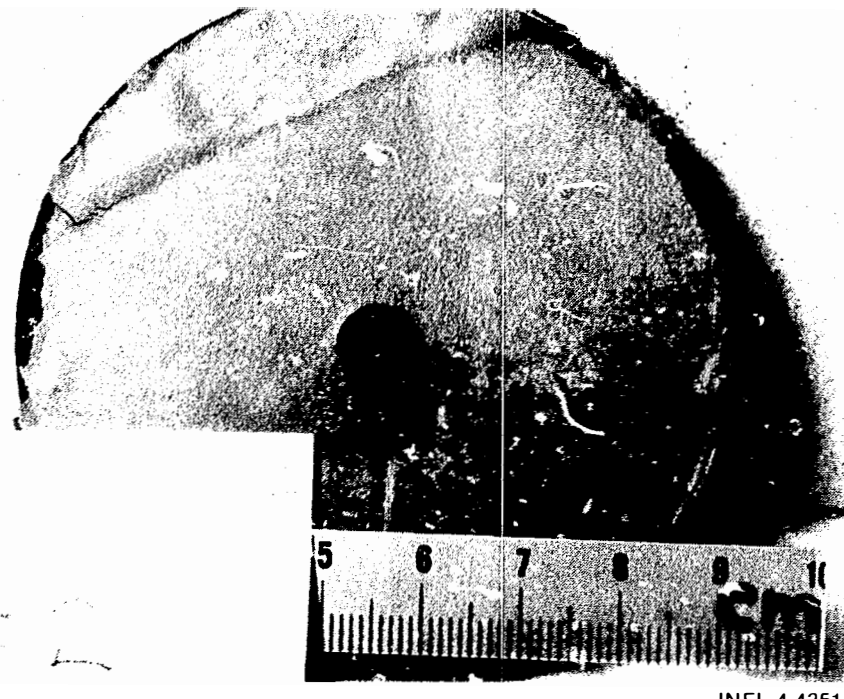
INEL 4 4371

Figure 26. Photomicrograph normal to the interior surface of Section 2 from liner PF-3 showing a cross section through a coating layer.



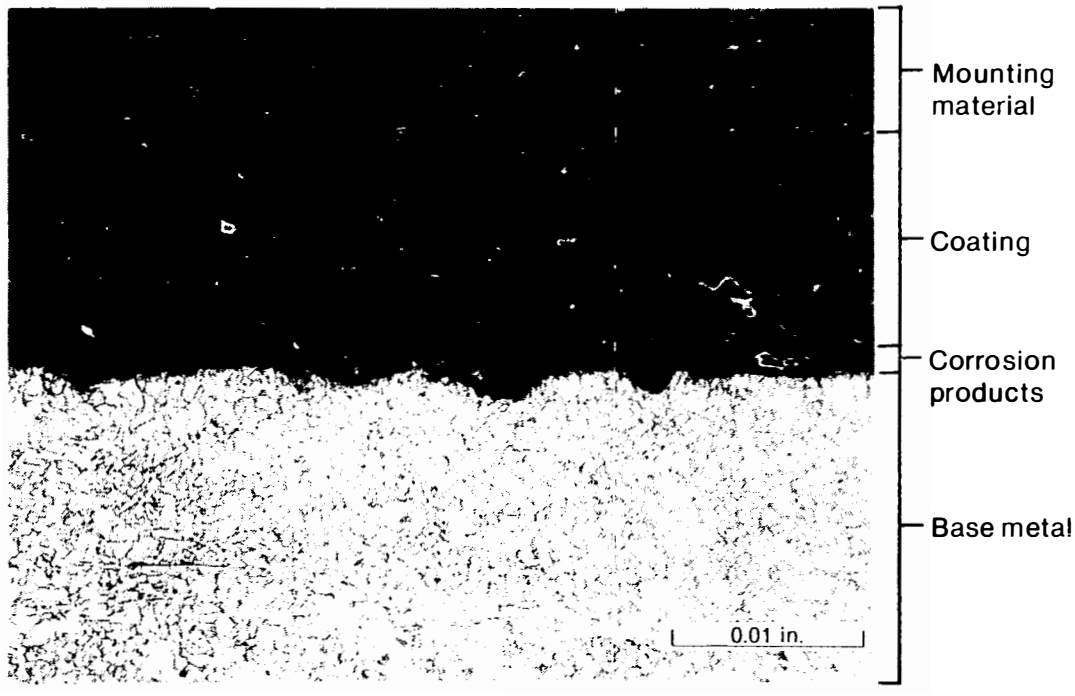
INEL 4 4337

Figure 27. Photomicrograph normal to the interior surface of Section 2 from liner PF-3 showing corrosion products adhering to the base metal and not the coating.



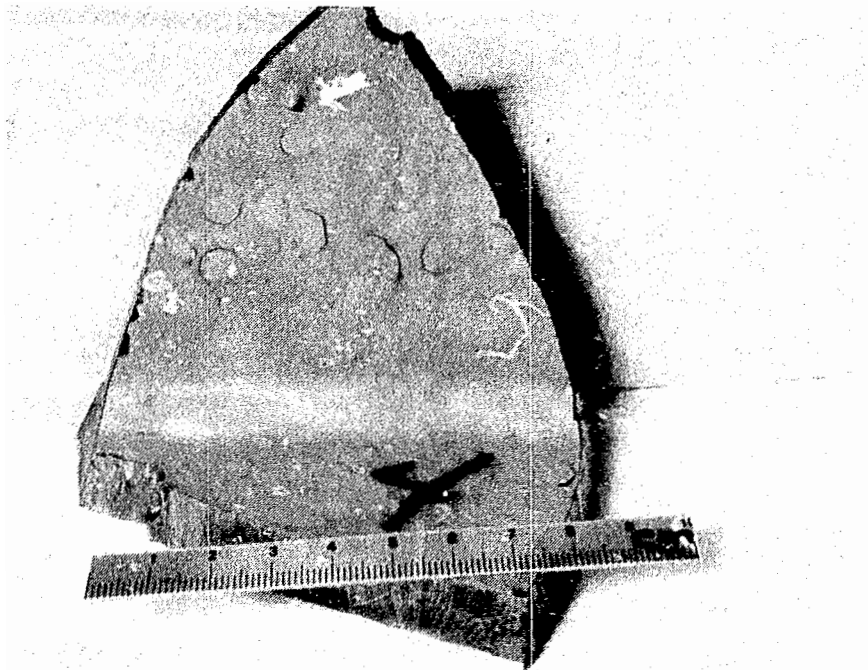
INEL 4 4351

Figure 28. Photograph of the interior surface of Section 2 from liner PF-16 showing a nearly defect-free coating.



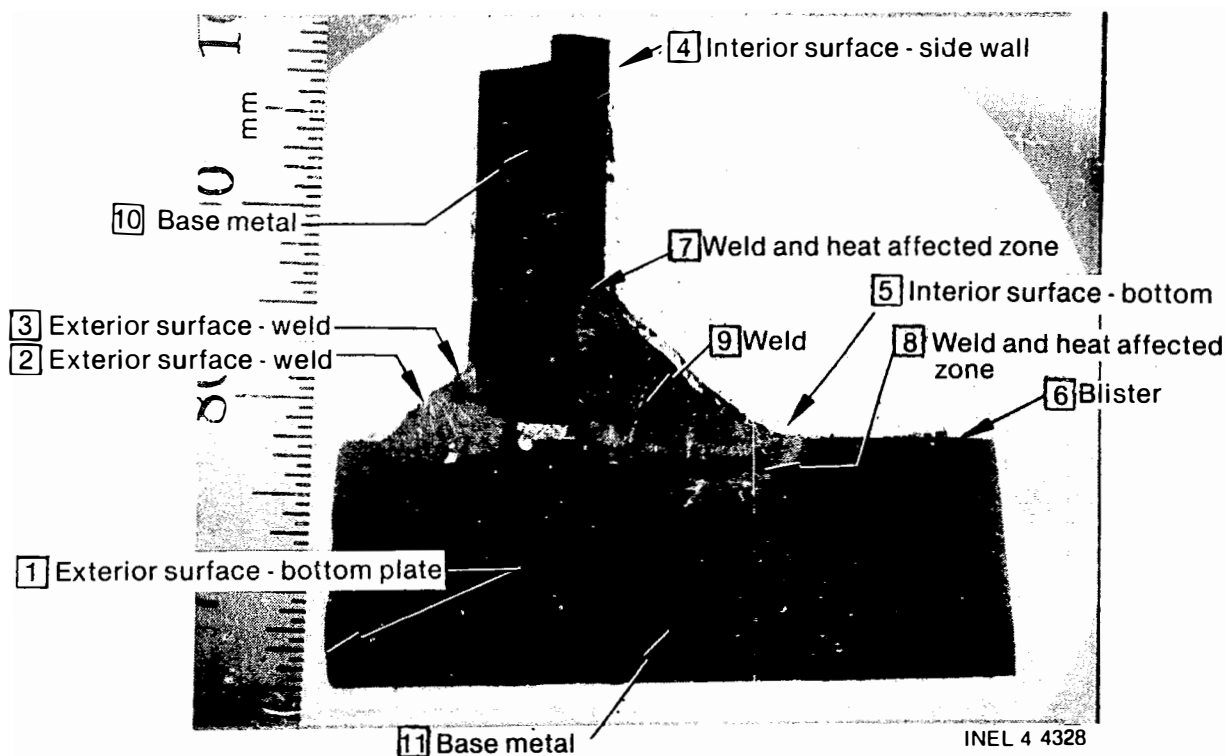
INEL 4 4346

Figure 29. Photomicrograph normal to the interior surface of Section 2 from liner PF-16 showing corrosion products between the coating and base metal.



INEL 4 4342

Figure 30. Photograph of Section 4 from liner PF-16 showing blisters on the interior surfaces of both the bottom and sidewall of the liner.



INEL 4 4328

Figure 31. Photograph of vertical section (Section 4 from liner PF-16) through the bottom plate to sidewall joint showing loose coating on the internal wall and surfaces of the welds. Note that the weld joints were not prepared prior to welding, and the welds were made with single passes for both the outside and the inside weld fillets. Location of metallurgical specimens from Section 4 are indicated.

between the bottom plate and wall of the liner. Corrosion products are evident between the coating and base metal on both the interior and exterior coated surfaces of the liner.

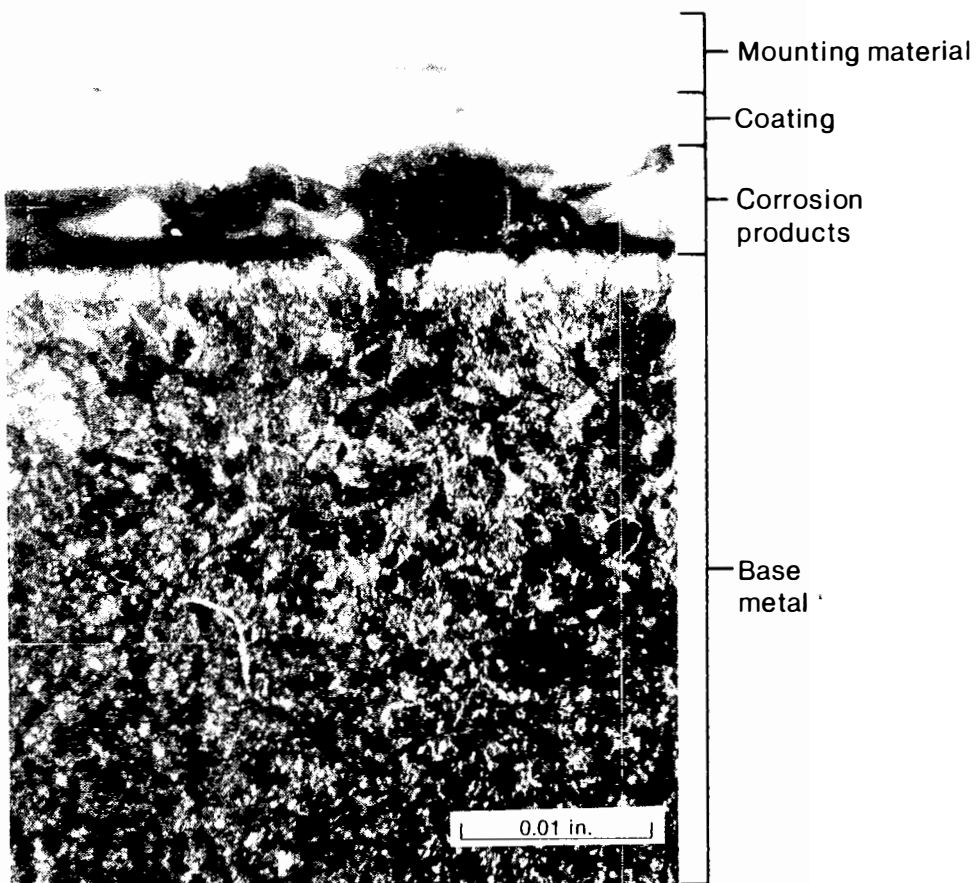
Section 4, Specimen 1--Examination of Specimen 1 (taken from the outside edge of the bottom plate) using polarized light revealed corrosion products between the coating and base metal (Figure 32). The corrosion products are about 0.004-in. thick and the exterior coating is about 0.005-in. thick.

Section 4, Specimens 2 and 3--Specimens 2 (Figure 33) and 3 (Figure 34) were prepared from the unexposed surfaces of the exterior weld between the bottom and wall of the liner. They were examined using polarized light. Porosity in the coating extended to the base metal through the corrosion products, which indicates that the coating had been applied over the corrosion products (Figure 33). Corrosion products extending into the coating were observed on the external weld surface (Figure 34).

Section 4, Specimen 4--When Specimen 4 was examined using polarized light, a heavy coating (about 0.020-in. thick) and surface gouges or scratches in the base metal were evident on the inside surface of the sidewall (Figure 35). Nonadherent corrosion products (from 0.002 to 0.004-in. thick) were evident between the coating and base metal.

Section 4, Specimen 5--Examination of Specimen 5 using polarized light revealed a separation between the coating and surface of the weld metal (Figure 36). Some nonadherent corrosion products were observed in that separation.

Section 4, Specimen 6--Surface discontinuities and large void areas were observed under the blister on Specimen 6, which was prepared from the inside of the bottom plate (Figure 37). The surface discontinuities indicate that the base metal had been gouged during fabrication.



INEL 4 4341

Figure 32. Photomicrograph normal to the exterior of Section 4, Specimen 1 from liner PF-16 showing corrosion products between the coating and base metal (specimen illuminated with polarized light).

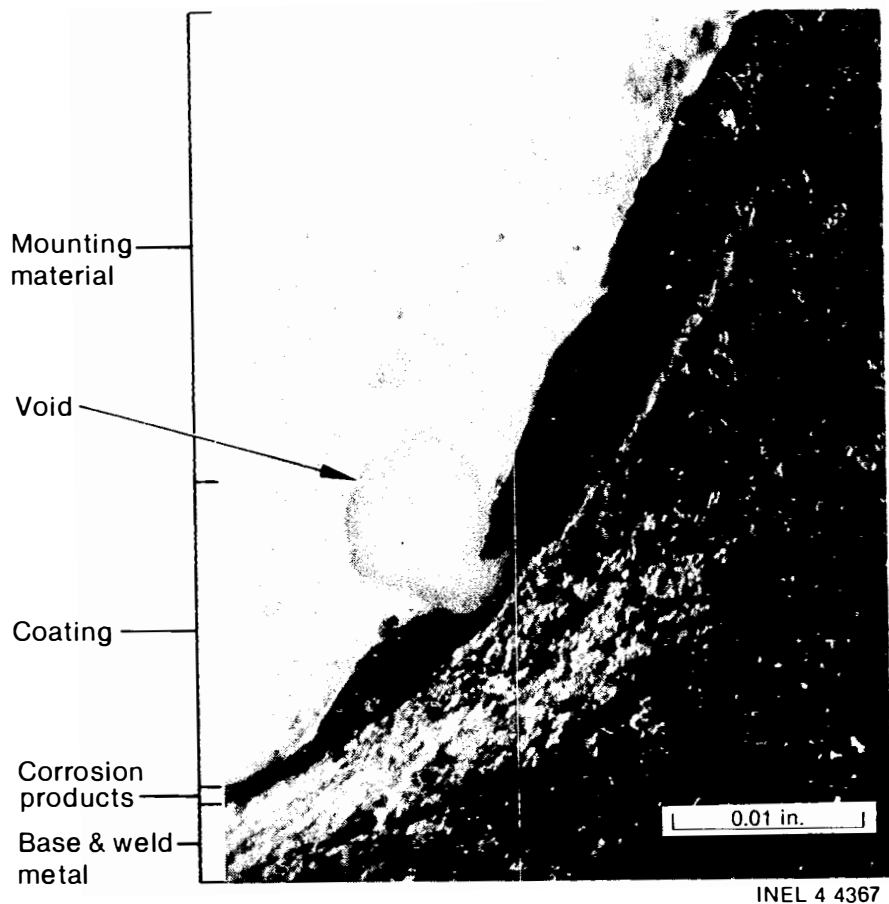


Figure 33. Photomicrograph of Section 4, Specimen 2 from liner PF-16 (made normal to the exterior weld surface) showing corrosion products between the coating and weld fillet and porosity in the coating (specimen illuminated with polarized light).

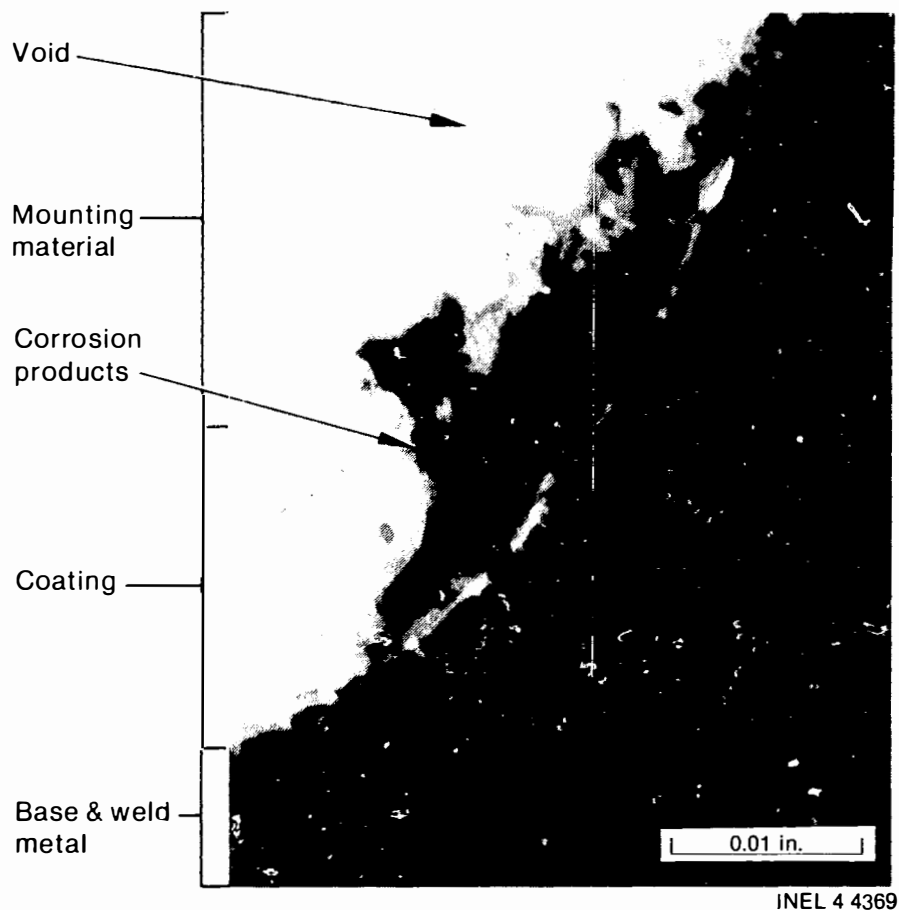
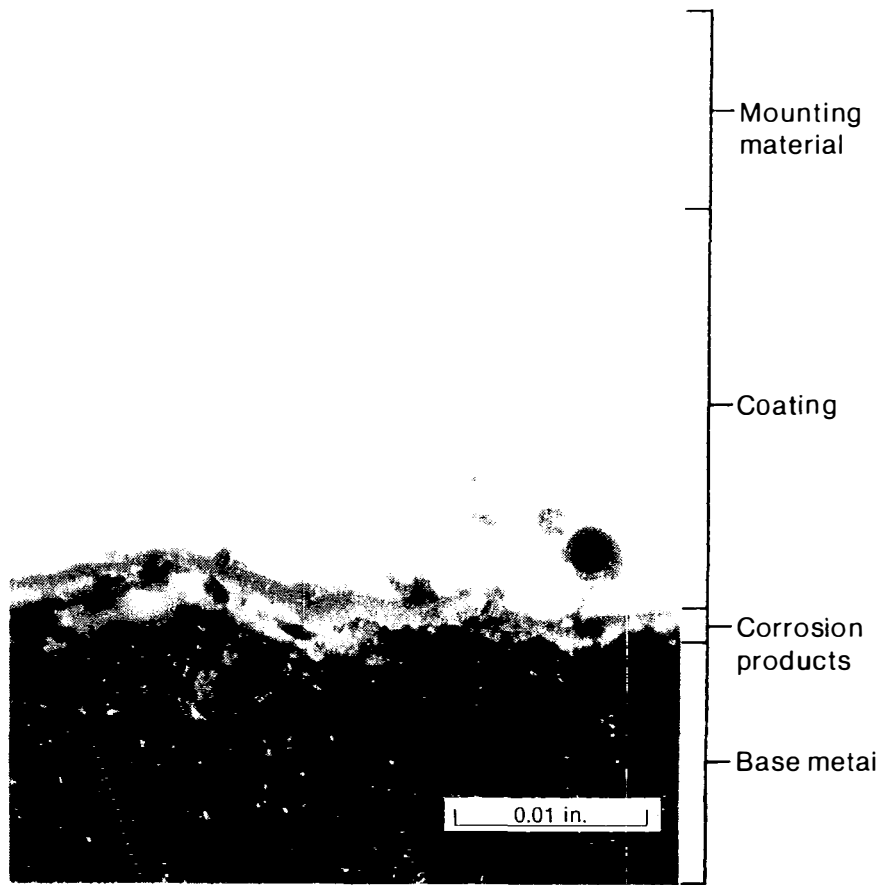


Figure 34. Photomicrograph of Section 4, Specimen 3 from liner PF-16 (made normal to the exterior weld surface) showing corrosion products at the weld surface extending into the coating (specimen illuminated with polarized light).



INEL 4 4368

Figure 35. Photomicrograph of Section 4, Specimen 4 from liner PF-16 (made normal to the interior surface of the sidewall) showing a heavy coating, corrosion products between the coating and base metal, and a surface gouge or scratch in the base metal (specimen illuminated with polarized light).

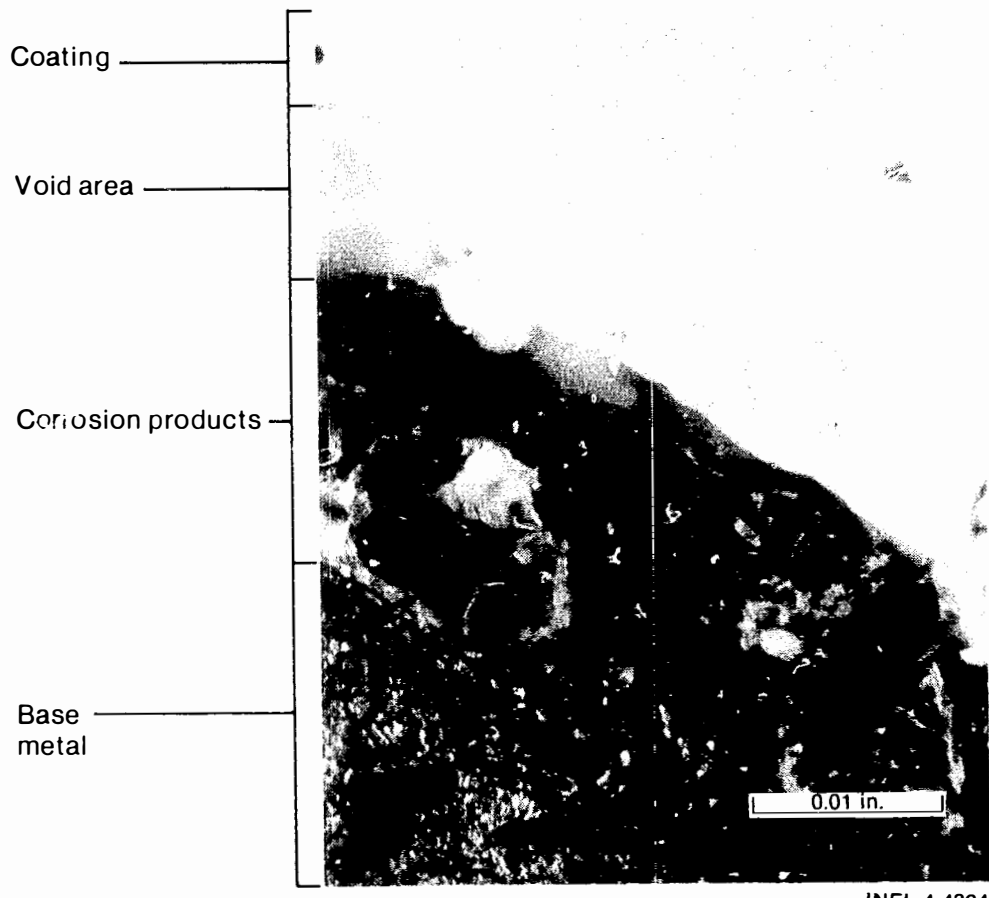


Figure 36. Photomicrograph of Section 4, Specimen 5 from liner PF-16 (made normal to the interior weld surface) showing separation between the coating and surface of the weld. Some corrosion products are evident in the separation (specimen illuminated with polarized light).

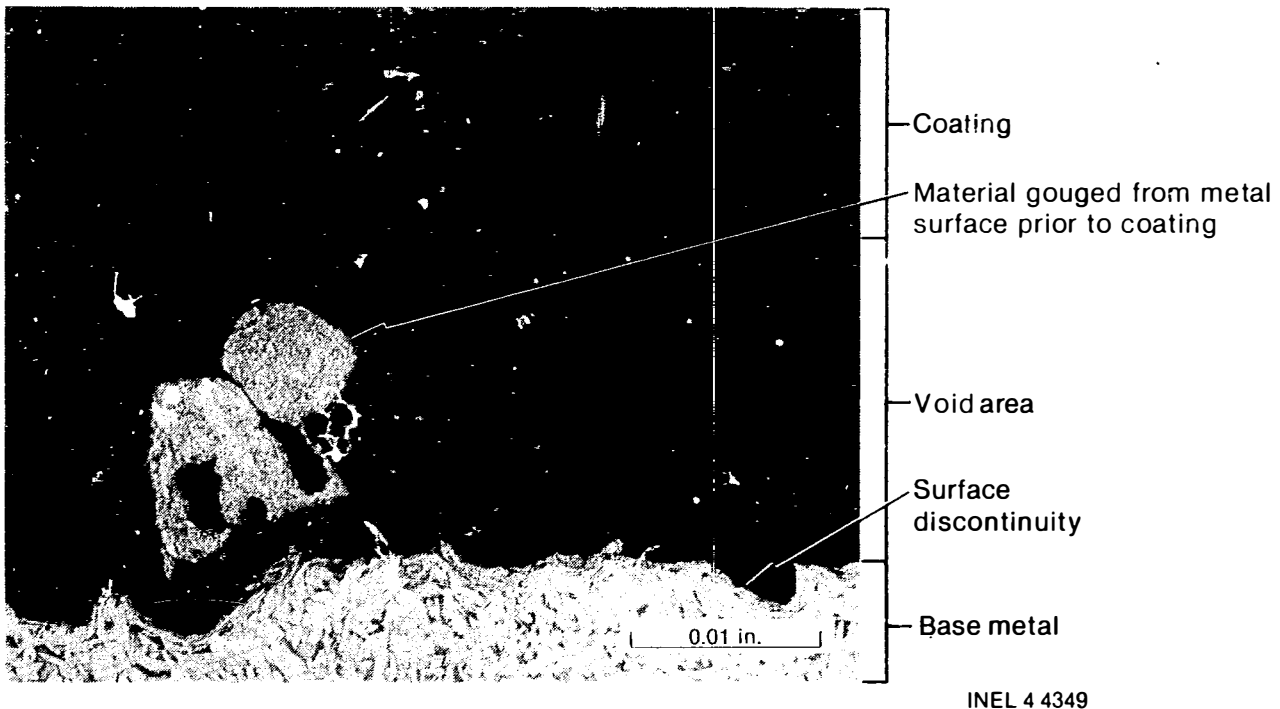


Figure 37. Photomicrograph of Section 4, Specimen 6 from liner PF-16 (made normal to the interior surface of the bottom plate) showing surface discontinuities and large void areas under the blister between the coating and the base metal.

Section 4, Specimens 7 and 8--Examination of specimens from the heat affected zones and weld deposits in the liner wall (Specimen 7, Figure 38) and bottom plate (Specimen 8, Figure 39) revealed dark spheres in the weld deposit, which are voids or nonmetallic inclusions.

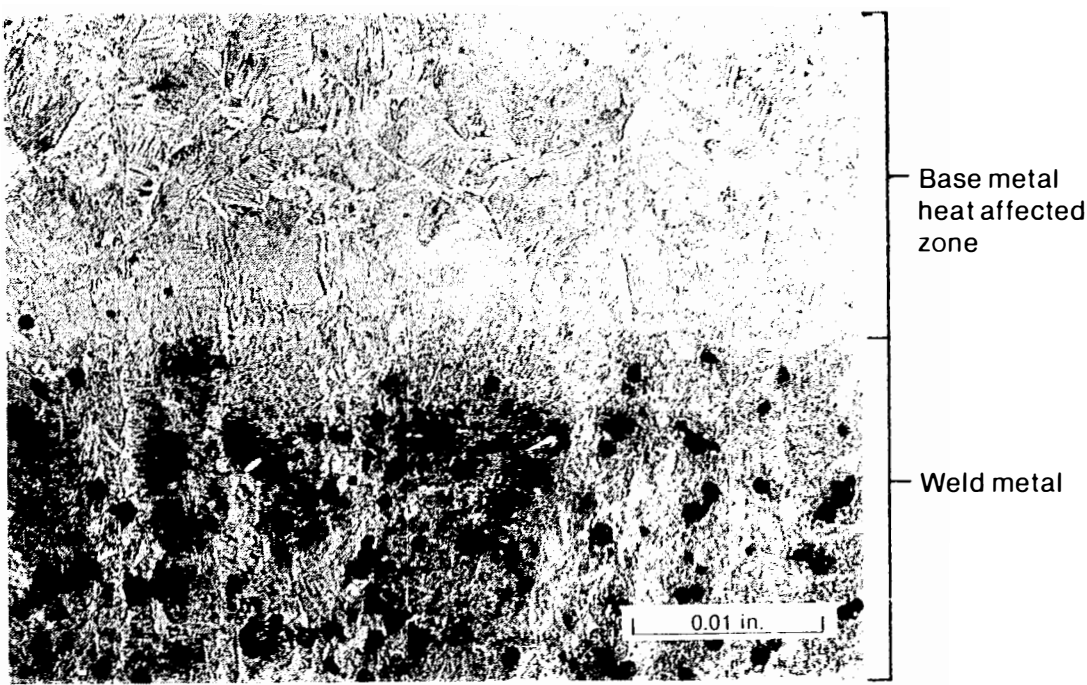
Section 4, Specimen 9--Dark spheres in the weld deposit of Specimen 9 are voids and nonmetallic inclusions (Figure 40). The void areas probably contained nonmetallic inclusions that were pulled out during the polishing operation of specimen preparation. The nonmetallic inclusions seem to be flux entrapment defects and are similar in appearance to flux entrapment defects observed in other carbon steel weldments.

Section 4, Specimen 10--Examination of the wall of liner PF-16 (Specimen 10) revealed a normal fine-grained (ASTM grain size No. 8 or finer) structure (Figure 41).

Section 4, Specimen 11--Examination of the bottom plate of liner PF-16 (Specimen 11) revealed a fine-grained (ASTM duplex grain size No. 6 to 8) structure (Figure 42).

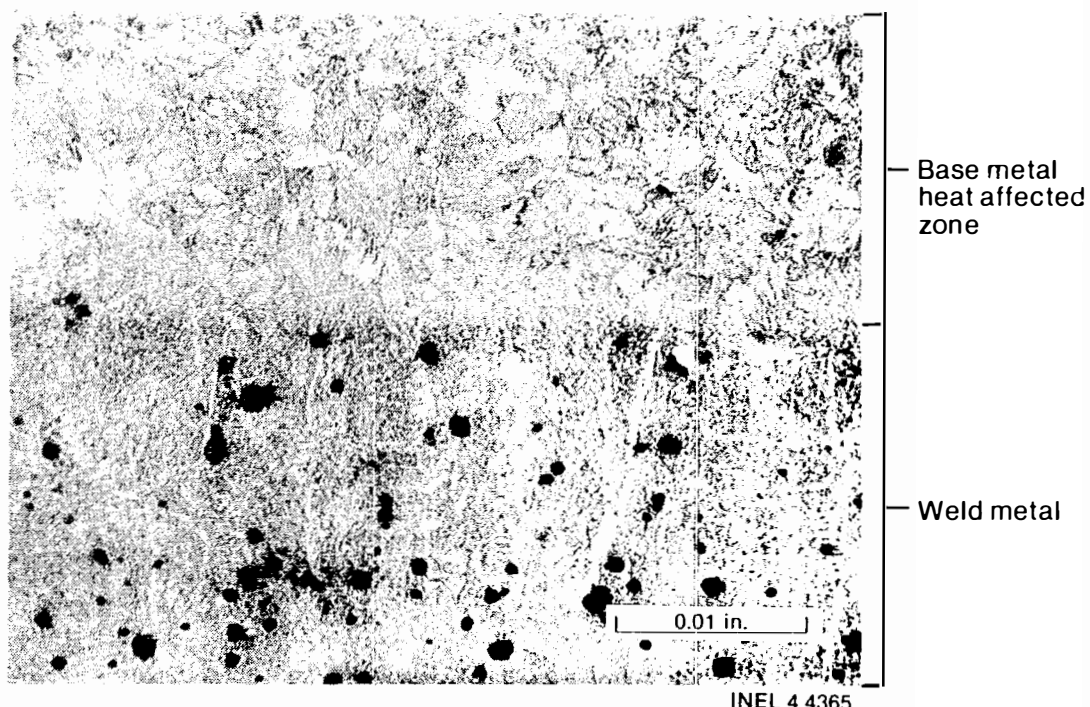
Section 5. Section 5 was removed from the lower sidewall of liner PF-16, about 8-in. above the ~~bottom~~, 120-degrees counterclockwise from the manway (see Figure 3). Visual examination of the interior surface of that section (Figure 43) revealed a comparatively adherent coating and several small blisters on the coating surface.

Section 5, Specimen 1--Examination of Specimen 1 revealed some corrosion products (about 0.0015-in. thick) between the coating and base metal and a coating thickness of about 0.010 in. (Figure 44). Further examination using polarized light (Figure 45) revealed coating (light colored material) between the corrosion products (medium dark lines) and base metal (dark granular area), which indicates that the coating had been applied over the corrosion products.



INEL 4 4340

Figure 38. Photomicrograph of Section 4, Specimen 7 from liner PF-16 showing the heat affected zone in the liner wall and weld deposit. The dark spheres are voids or nonmetallic inclusions in the weld deposit.



INEL 4 4365

Figure 39. Photomicrograph of Section 4, Specimen 8 from liner PF-16 showing the heat affected zone in the liner bottom plate and weld deposit. The dark spheres are voids or nonmetallic inclusions in the weld deposit.

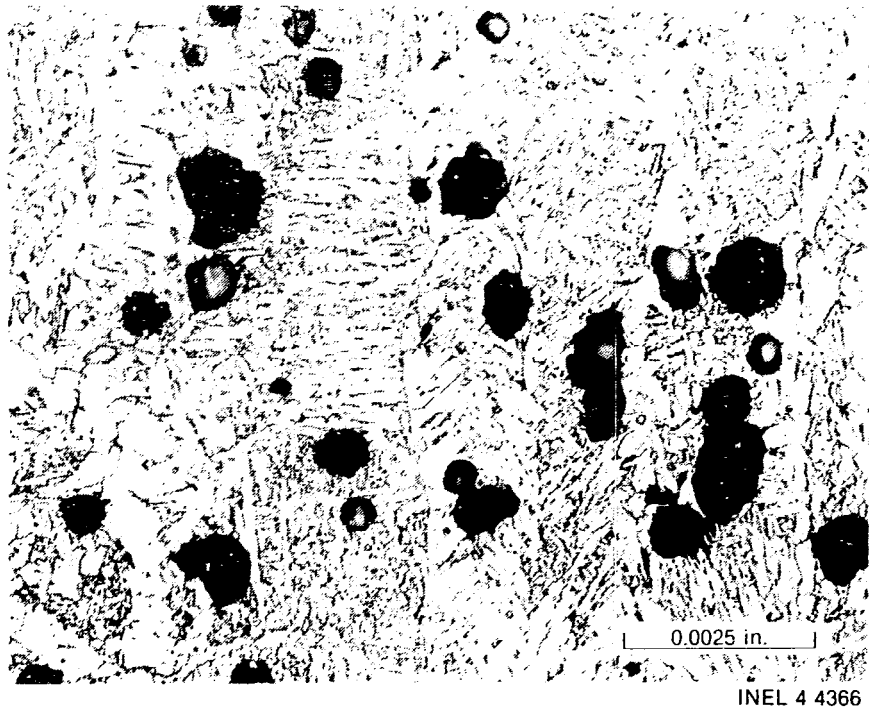


Figure 40. Photomicrograph of Section 4, Specimen 9 from liner PF-16 showing voids and nonmetallic inclusions at the center of the inner weld.

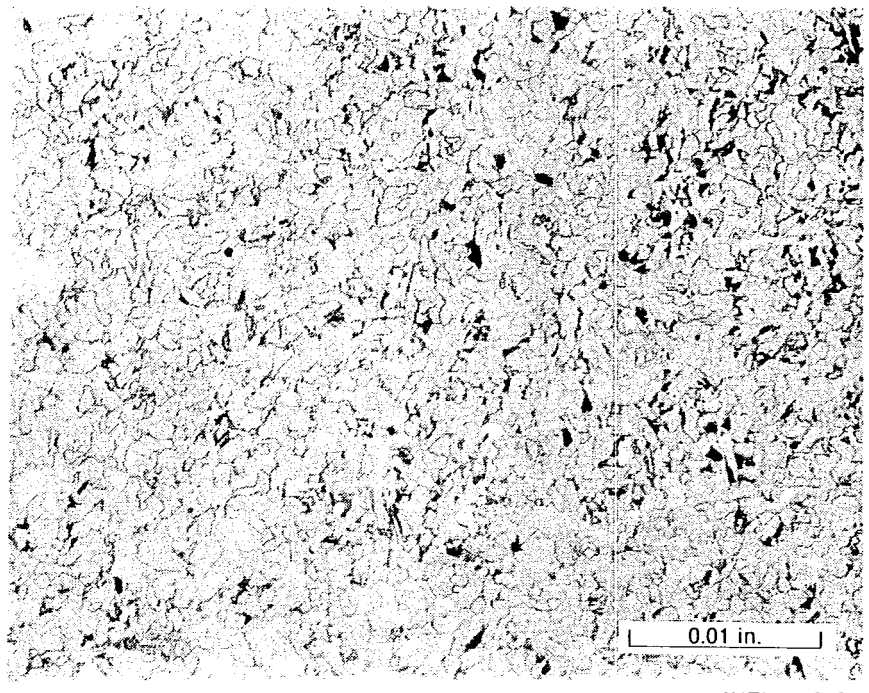


Figure 41. Photomicrograph taken from the liner wall of Section 4, Specimen 10 from liner PF-16 showing a fine-grained (ASTM grain size No. 8 or finer) base metal.



Figure 42. Photomicrograph of the base metal taken from the bottom plate of Section 4, Specimen 11 from liner PF-16 showing pearlitic (black) and ferritic (white) structures (ASTM duplex grain size No. 6 to 8).

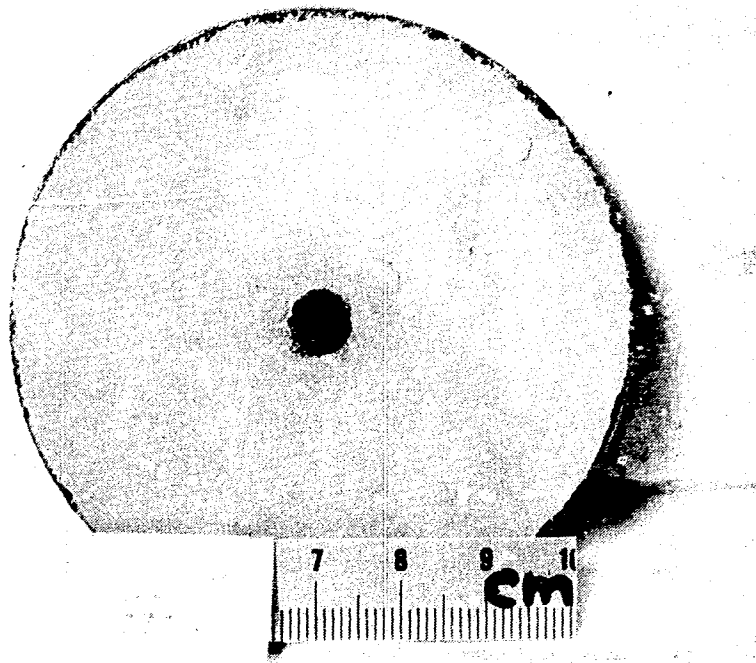
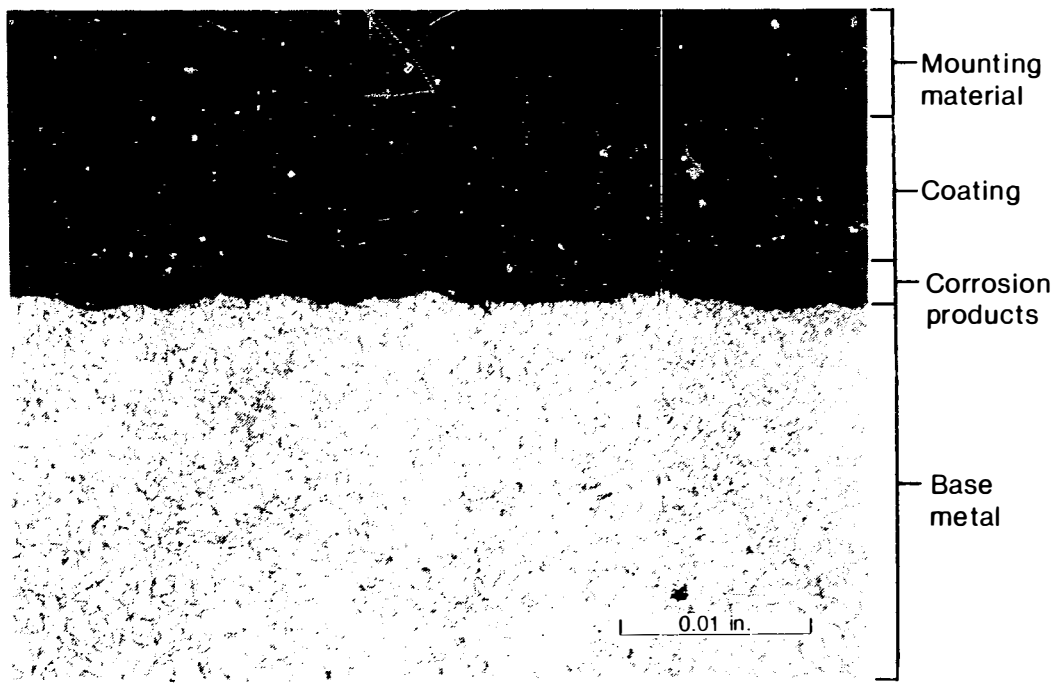
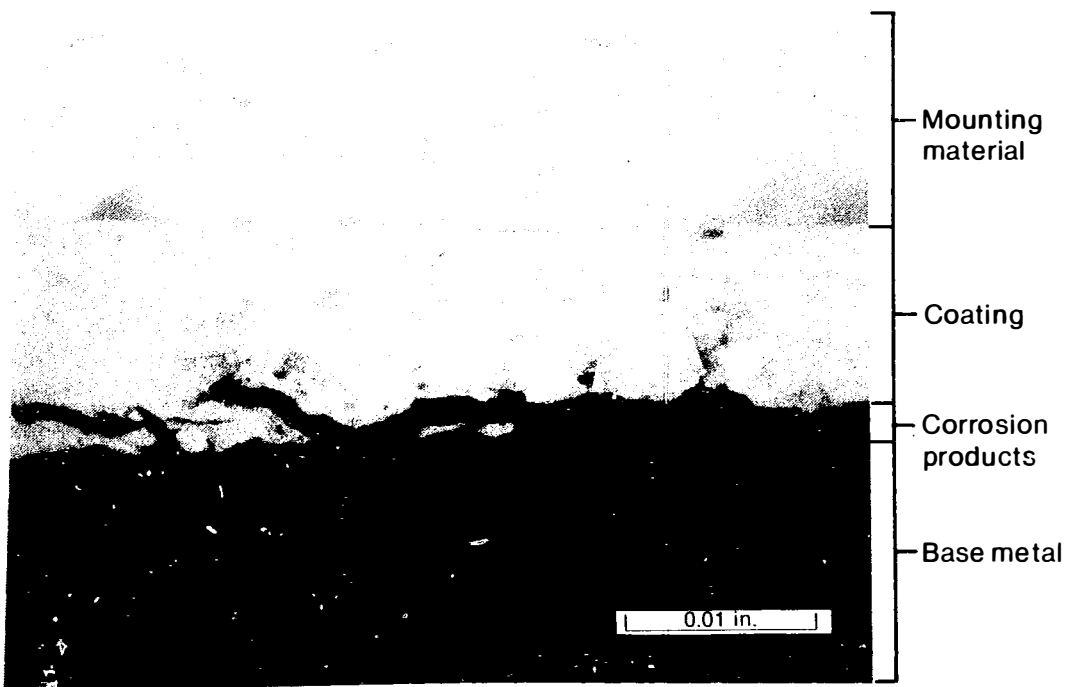


Figure 43. Photograph of the interior surface of Section 5 from liner PF-16 showing an adherent, nearly defect-free coating.



INEL 4 4350

Figure 44. Photomicrograph normal to the internal surface of Section 5 from liner PF-16 showing some corrosion products between the coating and base metal interface.



INEL 4 4359

Figure 45. Photomicrograph normal to the internal surface of Section 5 from liner PF-16 showing coating between the base metal and corrosion products (specimen illuminated with polarized light).

Section 6. Section 6 was removed from the lower sidewall of liner PF-16, about 2 in. from the bottom of the liner, 15-degrees clockwise from the manway (see Figure 3). The section was located at a large spalled area. Visual examination of the interior surface of the section revealed coating blisters and areas where the coating had spalled off, thereby exposing corrosion products on the surface of the base metal (Figure 46).

Section 6, Specimen 1--Examination of Specimen 1 revealed a coating thicknesses of about 0.012 in. on the interior surface and 0.010 in. on the exterior surface of the liner were measured (Figure 47). A blister is evident on the interior surface coating, while the external coating is not adhering to the base metal. Examination (using polarized light) revealed corrosion products adhering to the base metal between the coating and the base metal (Figure 48). Figure 49 shows the interior surface of the liner where the coating has spalled from the base metal. That area is nearly covered with adherent corrosion products, and a surface discontinuity is evident at the right of the figure. Figure 50 shows the discontinuity, which is a gouge or ding that occurred during fabrication, at 400 magnification.

Corrosion products on Specimen 1 are from 0.0005 to 0.002-in. thick. Four representative samples of apparent corrosion products from Specimen 1 were examined using electron discharge spectroscopy (EDS). It was determined that those products contained over 95% iron oxide, which confirmed that the material resulted from corrosion of the liner base metal.

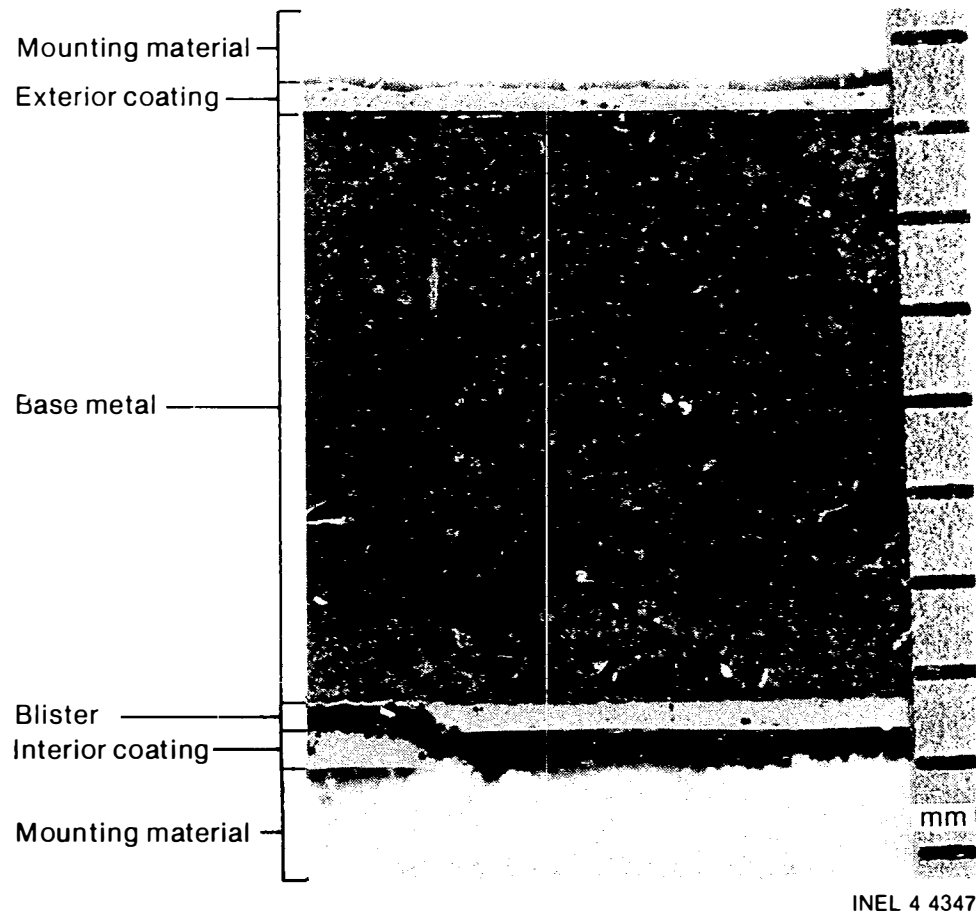
#### Discussion of Results

#### Coating Failure

The thickness of coatings on the internal and external surfaces of both liners varies considerably as shown in Table 3. The thickness of the exterior coating on specimens from liner PF-3 ranges from 0.009 to 0.012 in., and the interior coating from 0.005 to 0.009 in. The thickness of the exterior coating on specimens from liner PF-16 ranges from 0.005 to



Figure 46. Photograph of the interior surface of Section 6 from liner PF-16 showing blisters and exposed base metal.



INEL 4 4347

Figure 47. Photomicrograph normal to the wall of Section 6 from liner PF-16 showing coating on the interior surface (bottom) and exterior surface (top). The coating at bottom left is breeched at the edge of a blister.

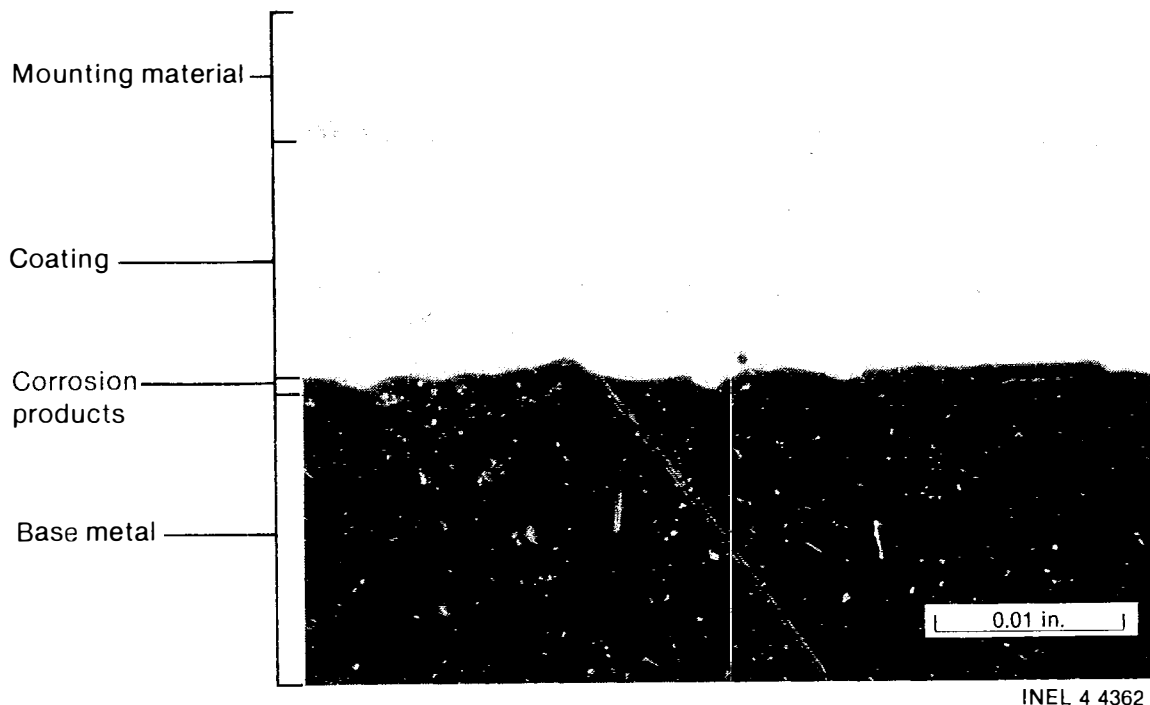


Figure 48. Photomicrograph normal to the internal surface of Section 6 from liner PF-16 showing corrosion products between the coating and base metal (specimen illuminated with polarized light).

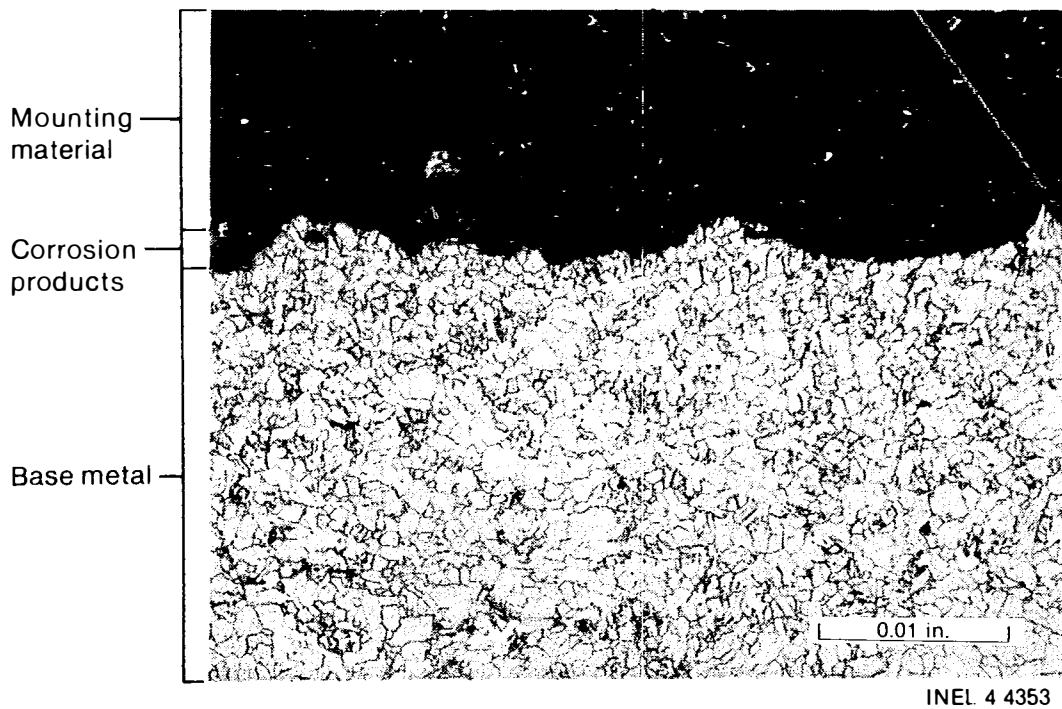


Figure 49. Photomicrograph normal to the internal surface of Section 6 from liner PF-16 showing corrosion products in an area where coating has spalled. Note discontinuity at right edge.

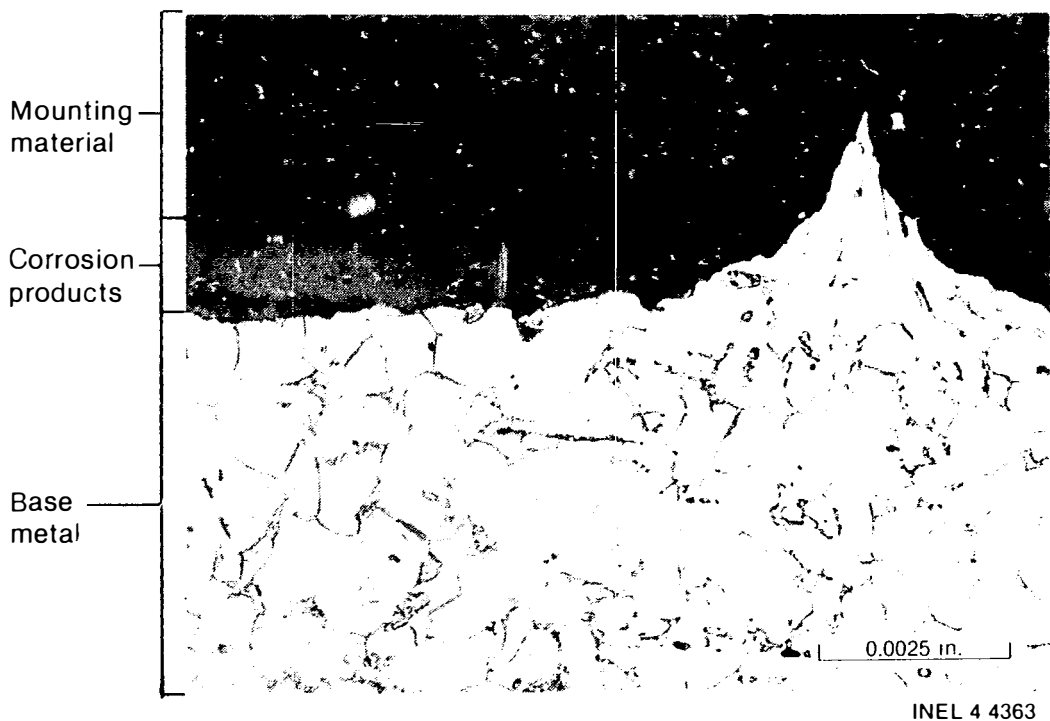


Figure 50. Photomicrograph showing greater detail of the discontinuity identified in Figure 49.

0.010 in., and the interior coating from 0.010 to 0.020 in. Coating failures are located primarily on interior surfaces of both liners, with the exception of those noted on the specimens from the bottom-to-sidewall weld area on the exterior surface of liner PF-16. Visual examination of both liners indicated that the coating on liner PF-3 was in better condition than that on PF-16. Coating thickness measurements show little difference between PF-3 and -16. Failures of the coatings (and especially the coating of PF-16) occurred in the area of the ion-exchanger bed. The more extensive coating damage observed in liner PF-16 can be attributed to the acidity of the water processed through that prefilter. The pH of the water processed through prefilter PF-16 was about 3, compared with a pH of about 7 for water processed through prefilter PF-3. The thickness of the coating adjacent to the blisters and spalled areas was about the same as that of adherent coating. The thicknesses of the coatings on the test plates were determined to be 0.011 to 0.012 in. No correlation can be made between coating thickness and extent of damage observed in the coating and base metal.

TABLE 3. COATING THICKNESS OF EPICOR-II LINERS PF-3 and PF-16 AND TEST PLATES 1 AND 1A

<u>Liner</u>	<u>Section</u>	<u>Thickness of External Coating (in.)</u>	<u>Thickness of Internal Coating (in.)</u>
PF-3	1	0.010	None
	2	0.009 - 0.012	0.006 - 0.009
	3	0.009 - 0.010	0.005
PF-16	2	0.005 - 0.007	0.012 - 0.014
	4	0.005	0.020
	5	Not photographed	0.010
	6	0.010	0.012
Test Plate 1		Not coated	0.011
Test Plate 1A		Not coated	0.012

Corrosion products were found between the coatings and the base metal on both the interior and exterior surfaces of both liners. In general, the corrosion products and coatings adhered to the base metal. Areas were observed where corrosion products were surrounded by coating, which suggests that corrosion products were formed before the coating was applied to the liner.

Differences in thickness were observed between corrosion products found under the adherent coating and corrosion products found under some of the interior blisters. Table 4 summarizes the amount of corrosion measured from photomicrographs included in this report. In general, corrosion products are thicker under the blisters than on the bare surfaces or under adherent coatings. It also was determined that corrosion products under the adherent coatings are from 0.0005 to 0.0015-in. thick. That thickness compares closely with the thickness of corrosion products found on the bare metal surfaces. It appears that the coating detached from the inner surfaces of the liners, cracked, and spalled off, resulting in the bare areas. The blisters were caused by a similar process, but the coating did not spall. The blisters allowed moisture to penetrate the coating to the base metal and thus promoted further corrosion product buildup, which the blister retained from erosion or sluffing. The total corrosion product thickness on the bare grounding area for the conductivity probe (shown in Figure 16 and listed in Table 4) was not measurable, because some of the corrosion products fell off during sample preparation.

Some coating failures observed on the interiors of both liners PF-3 and -16 are attributed to improper base metal surface preparation before coating. Radiation also was examined as a possible cause of failure. Radiation doses to the coatings on the internal surfaces of both liners were estimated at less than  $10^8$  rad. Tests performed on Phenoline coatings by Oak Ridge National Laboratory established limiting radiation resistance dose ratings.<sup>7</sup> Those limiting doses ranged from  $2.1 \times 10^9$  to  $8.3 \times 10^9$  rad for Phenoline 368 coating systems in demineralized water. Since the estimated doses for liners PF-3 and -16 are less than the limiting dose ratings, it can be stated that radiation damage was not the

cause of the coating failures. It also should be noted that the total estimated dose for the highest loaded liner after 13 years storage is about  $4 \times 10^3$  rad, which is below the limiting dose rating.

#### Base Metal Surface Condition

The surface conditions of liners PF-3 and -16 varied from smooth (with no discontinuities) to rough (with some gouges and dings). Metallographic examination of the exterior and interior base metal surfaces revealed that the surfaces were at least partially covered with a thin oxide layer of corrosion products. As noted in the discussion of Section 6 from PF-16, EDS examination verified that the layer was basically iron oxide.

TABLE 4. EPICOR-II LINER CORROSION THICKNESS

<u>Liner</u>	<u>Surface</u>	<u>Coating Condition</u>	<u>Figure</u>	<u>Corrosion Thickness (in.)</u>
PF-3	Interior	Bare	13	0.003 - 0.006 <sup>a</sup>
PF-3	Interior	Bare	16	0.002
PF-16	Interior	Bare	49	0.001 - 0.003
PF-3	Interior	Blister	26	0.004
PF-3	Interior	Blister	27	0.0005
PF-16	Interior	Blister	36	0.001 - 0.012
PF-16	Interior	Blister	35	0.002 - 0.004
PF-16	Interior	Blister	37	0.001 - 0.005
PF-16	Exterior	Blister	32	0.004
PF-16	Exterior	Blister	33	0.001 - 0.006
PF-16	Exterior	Blister	34	0.002 - 0.006
PF-3	Exterior	Adherent	18	0.0005
PF-3	Exterior	Adherent	19	0.0005
PF-3	Interior	Adherent	22	0.0005
PF-3	Interior	Adherent	23	0.0005
PF-3	Interior	Adherent	25	0.0005
PF-16	Interior	Adherent	29	0.001 - 0.0015
PF-16	Interior	Adherent	44	0.0015
PF-16	Interior	Adherent	45	0.001 - 0.0015
PF-16	Interior	Adherent	48	0.0005 - 0.001

a. Some corrosion products were lost during sample preparation.

A compilation of data obtained on the surface conditions of the base metals is shown in Table 5. The surface roughness levels on the two liners are compared with the roughness levels on the two test plates. The roughness levels on the liners are listed as smoother than, or similar to, the test plates. Review of the surface characteristics of liner PF-3 generally showed that those areas examined were smoother than the test plate surfaces. Surface characteristics of liner PF-16 showed that those areas examined were similar to the test plate surfaces. The comparison indicates that liner PF-3 had undergone a different surface preparation than PF-16, and that PF-16 had been given a surface preparation similar to that applied to the test plates. Examination of the uncoated surfaces of the test plates revealed rough finishes, which probably had been grit blasted before application of the coating. Metallographic examination of areas containing localized discontinuities indicates that those areas that were coated after being dinged or gouged had not corroded more than the adjacent base metal.

#### Calculation of Liner Minimum Lifetime

This section of the report presents a calculation of the minimum lifetime expected from an EPICOR-II liner. An area on the interior surface of each liner is bare. The bare area on liner PF-3 exhibited the minimum wall thickness for both liners. The metallurgical section removed from that area of PF-3 had a heavy buildup of corrosion products mixed with ion-exchange media on the surface. Table 2 compares base metal thicknesses of coated, uncorroded specimens from liner PF-3 with the base metal thicknesses of specimens from the uncoated, corroded bare area of that liner. Although it is known that some base metal was removed mechanically during removal of the coating from the grounding area, that loss of metal could not be identified separately from the amount of metal lost by corrosion. For that reason, in calculating the minimum lifetime of an EPICOR-II liner, it was assumed that all metal was lost by corrosion. It

TABLE 5. SURFACE CONDITION OF EPICOR-II LINER AND TEST PLATE BASE METAL

<u>Liner</u>	<u>Surface Location</u>	<u>Figure</u>	<u>Section</u>	<u>Description of Surface</u>
Test Plate 1	Coated	10	--	rough, coated
Test Plate 1A	Coated	11	--	rough, coated
PF-3	Interior	16	3	smoother than test plates, bare
	Exterior	18	3	smoother than test plates, coated <sup>a</sup>
	Exterior	19	3	smoother than test plates, coated
	Interior	22	2	smoother than test plates, coated <sup>a</sup>
	Interior	23	2	smoother than test plates, coated <sup>a</sup>
	Interior	25	2	smoother than test plates, coated
	Interior	26	?	smoother than test plates, blister
	Interior	27	2	smoother than test plates, blister
PF-16	Interior	29	2	rough, similar to test plates, coated
	Exterior	32	4	rough, similar to test plates, blister
	Interior	37	4	rough, similar to test plates, blister
	Interior	44	5	rough, similar to test plates, coated
	Interior	49	6	rough, similar to test plates, bare <sup>a</sup>

a. The surface exhibited a localized discontinuity.

also was assumed that the corrosion rate was, and will continue to be, linear using the analogy that the prefilter (i.e., liner wall, ion-exchange media, and water) was a flowing system. That was a conservative assumption because, although the prefilter was a flowing system during use, approximately three years of storage provided stagnant conditions. Also, the bare area is small compared with the total interior area of the liner in contact with resin (about 3%); that resulted in a maximum amount of base metal removal through corrosion by concentrating the total corrosion capability of the liner contents on that small area. The maximum thickness of uncorroded base metal from Section 3 of liner PF-3 is compared with the minimum thickness of corroded base metal from Section 1 of liner PF-3. That method will determine conservatively the minimum expected lifetime of a liner (assuming a uniform corrosion rate).

From Table 2:

maximum thickness of Section 3,  $x_3 = 0.2509$  in.

minimum thickness of Section 1,  $x_1 = 0.2346$  in.

gives

wall thickness loss,  $x = 0.0163$  in.

Then,

length of time between use and examination,  $t = 3.3$  yr

(31 October 1979 to 24 March 1983)

and

$$\text{corrosion rate, } R = \frac{x}{t} = \frac{0.0163 \text{ in.}}{3.3 \text{ yr}} = 0.005 \text{ in./yr}$$

gives

$$\text{minimum liner lifetime} = \frac{\text{nominal thickness}}{R} = \frac{0.250 \text{ in.}}{0.005 \text{ in./yr}} = 50 \text{ yr.}$$

The calculated minimum lifetime for a liner (50 years) exceeds the combined maximum planned interim storage period at INEL (10 years) and original storage period at TMI (3 years), for a total required life of 13 years. While 44 to 46 EPICOR-II liners presently stored at INEL will be disposed commercially within five years of original use at TMI, four to six liners will be retained at INEL for use in the ongoing resin research program.

#### Evaluation of Base and Weld Metal

The base metals of liners PF-3 (Figure 14) and PF-16 (Figures 41 and 42) are typical fine-grained structures. Abnormalities were not observed in those base metals.

Representative weld fillets between the bottom and sidewall of liner PF-16 are shown in Figure 31. There was no preparation of the weld joints, and a space exists between the welds. There was adequate penetration into the base metal, and the welds were sized adequately.

Examination of the welds in liner PF-16 revealed numerous small nonmetallic inclusions of entrapped flux (Figures 13 and 39). The observed defects are spherical and not linear or propagating-type defects; however, the number of voids and inclusions observed indicates that there were inadequate controls applied to the welding process.

## CONCLUSIONS

Visual and metallographic examination of sections removed from the liners of EPICOR-II prefilters PF-3 and -16 revealed that the coatings had been breached and some areas of the carbon steel liners were corroded. Uniform corrosion was observed between the coating and base metal and on the surface of the base metal where the coating had spalled off. Metallographic examinations at 100 and 400 magnifications did not detect pitting or pitting-type corrosion. Corrosion also was observed between the exterior of the liner wall and the exterior coating. Coating blisters were observed on the interior surfaces of both liners. No coating blisters were observed on the exterior surfaces of either liner. There were indications that the coatings in many areas had been applied over corrosion products, which indicates that the base metal had not been properly prepared before application of the coatings. Coating failure was determined not to be attributable to radiation damage.

The area of maximum corrosion on liner PF-3 was determined to be the bare area on the inside surface where coating was intentionally removed. Corrosion in that area was observed to be uniform with no evidence of pitting or pitting-type corrosion. Comparing the minimum measured wall thickness in that corroded area with the measured uncorroded base metal thickness resulted in a calculated minimum lifetime for liner PF-3 of 50 years. That exceeds the required liner interim storage life of 13 years at INEL. The grounding area for the conductivity probe was not examined on liner PF-16, but it is assumed that corrosion in that area would be similar to the amount and type of the corrosion observed in liner PF-3.

The resin transfer system developed at INEL to remove ion-exchange media from the study prefilters performed satisfactorily, demonstrating that difficult to handle mixtures such as those contained in the EPICOR-II prefilter can be transported with vacuum sluicing techniques.

## RECOMMENDATIONS

Information obtained during the liner integrity examination shows that EPICOR-II prefilters can be stored safely in the TAN-607 Hot Shop of INEL for ten years without danger of loss of integrity of the liner wall. While it is planned to transport 44 to 46 prefilters to a disposal site within three years, from four to six prefilters will remain stored at the TAN area for up to ten years for use in NRC sponsored resin research programs.

It is recommended that waste products from future TMI-2 activities be stored in containers procured to specifications defining engineering requirements for both the materials and processes used to fabricate the containers. It is further recommended that the specifications include a requirement for containers that incorporate protective nonmetallic coatings which prevents removal of coating from localized areas and ensures complete coverage of coating on all exposed surfaces. [Small uncoated areas can provide sites for accelerated localized corrosion attack.] Experience at INEL and in industry indicates that such a vessel will perform satisfactorily for long periods of time if the materials of construction and process variables are defined and controlled during fabrication. Surface preparation and coating application are important to coating success, as is protection of the coating from damage. Therefore vessels such as EPICOR-II prefilter liners can be constructed of carbon steel coated with nuclear grade phenolic or epoxy paint. The surfaces should be prepared for painting by grit blasting or as recommended by the coating manufacturer. The prepared surfaces then must be protected from corrosion until painted.

REFERENCE S

1. J. W. McConnell, EPICOR-II Resin/Liner Research Plan, EGG-TMI-6198, EG&G Idaho, Inc., March 1983.
2. J. D. Yesso, V. Pasupathi, L. Lowery, Battelle Memorial Institute Columbus Laboratories, Characterization of EPICOR-II Prefilter Liner 16, GEND-015, August 1982.
3. N. L. Wynhoff, V. Pasupathi, Battelle Memorial Institute Columbus Laboratories, Characterization of EPICOR-II Prefilter Liner 3, GEND-027, April 1983.
4. Program Plan for EPICOR-II Research and Disposition Program, EG&G Idaho, Inc., April 1982 (Revised September 1982).
5. H. W. Reno, R. L. Dodge, The EPICOR-II Research and Disposition Program at the INEL, EGG-M-19482, EG&G Idaho, Inc., 13 September 1982.
6. Personal Communication between C. Hitz, GPU Nuclear, and J. W. McConnell, EG&G Idaho, Inc., 13 May 1983.
7. ORNL-3916, Unit Operations Section Quarterly Progress Report, July-September 1965, Contract No. W-7405-ang-26, March 1966.

RECOMMENDATIONS .....	64
REFERENCES .....	65

GEND--037

DE84 003469

Distribution Category: UC-78

# **SURFACE ACTIVITY AND RADIATION FIELD MEASUREMENTS OF THE TMI-2 REACTOR BUILDING GROSS DECONTAMINATION EXPERIMENT**

**Charles V. McIsaac**

**Published October 1983**

**MASTER**

**EG&G Idaho, Inc.  
Idaho Falls, Idaho 83415**

**Prepared for the  
U.S. Department of Energy  
Three Mile Island Operations Office  
Under DOE Contract No. DE-AC07-76IDO1570**

*Approved by the U.S. Department of Energy* *[Signature]*

## ABSTRACT

Surface samples were collected from concrete and metal surfaces within the Three Mile Island Unit 2 Reactor Building on December 15 and 17, 1981 and again on March 25 and 26, 1982. The Reactor Building was decontaminated by hydrolasing during the period between these dates. The collected samples were analyzed for radionuclide concentration at the Idaho National Engineering Laboratory. The sampling equipment and procedures, and the analysis methods and results are discussed in this report.

The measured mean surface concentrations of  $^{137}\text{Cs}$  and  $^{90}\text{Sr}$  on the 305-ft elevation floor before decontamination were, respectively,  $3.6 \pm 0.9$  and  $0.17 \pm 0.04 \mu\text{Ci}/\text{cm}^2$ . Their mean concentrations on the 347-ft elevation floor were about the same. On both elevations, walls were found to be considerably less contaminated than floors. The fractions of the core inventories of  $^{137}\text{Cs}$ ,  $^{90}\text{Sr}$ , and  $^{129}\text{I}$  deposited on Reactor Building surfaces prior to decontamination were calculated using their mean concentrations on various types of surfaces. The calculated values for these three nuclides are  $3.5 \pm 0.4 \text{ E-4}$ ,  $2.4 \pm 0.8 \text{ E-5}$ , and  $5.7 \pm 0.5 \text{ E-4}$ , respectively.

The decontamination operations reduced the  $^{137}\text{Cs}$  surface activity on the 305- and 347-ft elevations by factors of 20 and 13, respectively. The  $^{90}\text{Sr}$  surface activity reduction was the same for both floors, that being a factor of 30. On the whole, decontamination of vertical surfaces was not achieved.

Beta and gamma exposure rates that were measured during surface sampling were examined to determine the degree to which they correlated with measured surface activities. The data were fit with power functions of the form  $y = ax^b$ . As might be expected, the beta exposure rates showed the best correlation. Of the data sets fit with the power function, the set of December 1981 beta exposure rates exhibited the least scatter. The coefficient of determination for this set was calculated to be 0.915.

## ACKNOWLEDGEMENTS

This sampling program was conducted as a joint effort of EG&G Idaho, General Public Utilities Nuclear Corporation (GPUNC)/Metropolitan Edison, and personnel of other technical companies providing support to GPUNC/Metropolitan Edison. The author gratefully extends thanks to the individuals from these organizations who collected surface samples during one or more Reactor Building entries.

The evolution of the surface sampler from a concept to a tangible tool came about because of the contributions made by a number of individuals. The conceptual design of the sampler was a fusion of ideas and suggestions offered by T. E. Cox, C. V. McIsaac, P. D. Randolph, and O. D. Simpson. The design engineering work was performed by W. M. Laney. Special thanks are extended to Bill Miller, owner of the K&M Machine and Tool Company, Hummelstown, Pennsylvania, and his staff for the extra effort they made when fabricating the two prototype samplers. D. M. Anderson, D. C. Hetzer, C. V. McIsaac, Bill Miller and S. V. Rodriguez were instrumental in testing and modifying the prototype samplers.

## DISCLAIMER

This report was prepared as an account of work sponsored by an agency of the United States Government. Neither the United States Government nor any agency thereof, nor any of their employees, makes any warranty, express or implied, or assumes any legal liability or responsibility for the accuracy, completeness, or usefulness of any information, apparatus, product, or process disclosed, or represents that its use would not infringe privately owned rights. Reference herein to any specific commercial product, process, or service by trade name, trademark, manufacturer, or otherwise does not necessarily constitute or imply its endorsement, recommendation, or favoring by the United States Government or any agency thereof. The views and opinions of authors expressed herein do not necessarily state or reflect those of the United States Government or any agency thereof.

## CONTENTS

ABSTRACT .....	ii
ACKNOWLEDGEMENTS .....	iii
INTRODUCTION .....	1
SAMPLING EQUIPMENT .....	2
Surface Sampler .....	2
Calibration .....	4
Gross Beta/Gamma Survey Instrument .....	6
SAMPLING PROCEDURE .....	8
ANALYSIS METHODS .....	11
RESULTS .....	13
DISCUSSION .....	15
Surface Activities .....	15
Decontamination Factors .....	18
Beta and Gamma Exposure Rates .....	20
REFERENCES .....	23
APPENDIX A--SAMPLING PROCEDURE .....	105
APPENDIX B--ANALYSIS METHODS .....	111

## FIGURES

1. Surface sampler and air pump schematic .....	24
2. Surface sampler vacuum chamber and milling bits schematic .....	25
3. Surface sampler sample filter cartridge schematic .....	26
4. Sample locations at the 305-ft elevation .....	27
5. Sample locations at elevations 347 ft-6-in. and above .....	28
6. December 1981 and March 1982 beta and gamma exposure rates, at the 305-ft elevation (shown on the 305-ft elevation floor plan) .....	29

7.	December 1981 and March 1982 beta and gamma exposure rates at elevations 347 ft,6 in., 367 ft,4 in., and 369 ft,6 in. (shown on the 347 ft,6 in. elevation floor plan) .....	30
8.	December 1981 Cs-137 surface concentration vs beta exposure rate .....	31
9	December 1981 Cs-137 surface concentration vs gamma exposure rate .....	32
10.	March 1982 Cs-137 surface concentration vs beta exposure rate .....	33
11.	March 1982 Cs-137 surface concentration vs gamma exposure rate .....	34
12.	December 1981 and March 1982 Cs-137 surface concentration vs beta exposure rate .....	35

#### TABLES

1.	Activity collection efficiencies of surface samplers for four types of surfaces .....	36
2.	Number of locations sampled at each Reactor Building elevation .....	37
3.	Masses of collected millings for post-decontamination samples .....	38
4.	Calculated depths of sampling--horizontal concrete .....	39
5.	Measured surface activity concentrations on the concrete floor at the 305-ft elevation within the TMI-2 Reactor Building listed by sample (decay-corrected to March 26, 1982) .....	40
6.	Measured surface activity concentrations on the D-ring wall at the 305-ft elevation within the TMI-2 Reactor Building listed by sample (decay-corrected to March 26, 1982) .....	43
7.	Measured surface activity concentrations on vertical metal at the 305-ft elevation within the TMI-2 Reactor Building listed by sample (decay-corrected to March 26, 1982) .....	44
8.	Measured surface activity concentrations on the concrete floor at the 347-ft elevation within the TMI-2 Reactor Building listed by sample (decay-corrected to March 26, 1982) .....	45

9.	Measured surface activity concentrations on metal decking at the 347-ft elevation within the TMI-2 Reactor Building listed by sample (decay-corrected to March 26, 1982) .....	48
10.	Measured surface activity concentrations on the D-ring wall at the 347-ft elevation within the TMI-2 Reactor Building listed by sample (decay-corrected to March 26, 1982) .....	49
11.	Measured surface activity concentrations on the cinderblock wall at the 347-ft elevation within the TMI-2 Reactor Building (decay-corrected to March 26, 1982) .....	50
12.	Measured surface activity concentrations on vertical metal surfaces at the 347-ft elevation within the TMI-2 Reactor Building (decay-corrected to March 26, 1982) .....	51
13.	Measured surface activity concentrations on the "A" D-ring wall walkway at the 347-ft elevation within the TMI-2 Reactor Building (decay-corrected to March 26, 1982) .....	52
14.	Measured surface activity concentrations on the RC-P-2A I beam, (horizontal) at the 369-ft elevation within the TMI-2 Reactor Building (decay-corrected to March 26, 1982) .....	53
15.	Measured surface activity concentrations on the RC-P-2A I beam (vertical) at the 369-ft elevation within the TMI-2 Reactor Building (decay-corrected to March 26, 1982) .....	54
16.	Measured surface activity concentrations on the elevator shaft roof at the 372-ft elevation within the TMI-2 Reactor Building (decay-corrected to March 26, 1982) .....	55
17.	Measured surface activity concentrations on the concrete floor at the 305-ft elevation within the TMI-2 Reactor Building listed by sampling location (decay-corrected to March 26, 1982) .....	56
18.	Measured surface activity concentrations on the D-ring wall at the 305-ft elevation within the TMI-2 Reactor Building (decay-corrected to March 26, 1982) .....	58
19.	Measured surface activity concentrations on vertical metal surfaces at the 305-ft elevation within the TMI-2 Reactor Building (decay-corrected to March 26, 1982) .....	59
20.	Measured surface activity concentrations on the concrete floor at the 347-ft elevation within the TMI-2 Reactor Building (decay-corrected to March 26, 1982) .....	60
21.	Measured surface activity concentrations on the concrete floor at the 347-ft elevation within the TMI-2 Reactor Building (decay-corrected to March 26, 1982) .....	61

22. Measured surface activity concentrations on metal decking at the 347-ft elevation within the TMI-2 Reactor Building (decay-corrected to March 26, 1982) .....	62
23. Measured surface activity concentrations on the D-ring wall at the 347-ft elevation within the TMI-2 Reactor Building (decay-corrected to March 26, 1982) .....	63
24. Measured surface activity concentrations on the cinderblock wall at the 347-ft elevation within the TMI-2 Reactor Building (decay-corrected to March 26, 1982) .....	64
25. Measured surface activity concentrations on vertical metal surfaces at the 347-ft elevation within the TMI-2 Reactor Building (decay-corrected to March 26, 1982) .....	65
26. Measured surface activity concentrations on the "A" D-ring walkway at the 367-ft elevation within the TMI-2 Reactor Building (decay-corrected to March 26, 1982) .....	66
27. Measured surface activity concentrations on the RC-P-2A I beam (horizontal) at the 367-ft elevation within the TMI-2 Reactor Building (decay-corrected to March 26, 1982) .....	67
28. Measured surface activity concentrations on the RC-P-2A I beam (vertical) on the 369-ft elevation within the TMI-2 Reactor Building (decay-corrected to March 26, 1982) .....	68
29. Measured surface activity concentrations on the elevator shaft roof at the 372-ft elevation within the TMI-2 Reactor Building (decay-corrected to March 26, 1982) .....	69
30. December 1981 mean Cs-137 surface concentrations listed by type of surface and elevation .....	70
31. December 1981 mean Cs-134 surface concentrations listed by type of surface and elevation .....	71
32. December 1981 mean Sr-90 surface concentrations listed by type of surface and elevation .....	72
33. December 1981 mean I-129 surface concentrations listed by type of surface and elevation .....	73
34. December 1981 mean Sb-125 surface concentrations listed by type of surface and elevation .....	74
35. December 1981 mean surface concentrations of several nuclides listed by type of surface and elevation .....	75
36. Mean values for each type of surface of the ratios of the December 1981 surface concentrations of several radionuclides to the concentration of Cs-137 measured in each surface sample .....	76

37. March 1982 mean Cs-137 surface concentrations listed by type of surface and elevation .....	78
38. March 1982 mean Cs-134 surface concentrations listed by type of surface and elevation .....	79
39. March 1982 mean Sr-90 surface concentrations listed by type of surface and elevation .....	80
40. March 1982 mean I-129 surface concentrations listed by type of surface and elevation .....	81
41. March 1982 mean Sb-125 surface concentrations listed by type of surface and elevation .....	82
42. March 1982 mean surface concentrations of several nuclides listed by type of surface and elevation .....	83
43. Mean Values for each type of surface of the ratios of the March 1982 surface concentrations of several radionuclides to the concentration of Cs-137 measured in each surface sample .....	84
44. December 15 and 17, 1981, beta and gamma exposure rates measured at surface sampling locations inside the TMI-2 Reactor Building .....	86
45. March 25 and 26, 1982, beta and gamma exposure rates measured at surface sampling locations inside the TMI-2 Reactor Building .....	88
46. Mean December 1981 and March 1982 beta and gamma exposure rates listed by surface type and elevation .....	90
47. Measured decontamination factors for loose and fixed Cs-137 surface activity listed by Reactor Building elevation and sampling location .....	91
48. Measured decontamination factors for loose and fixed Sr-90 surface activity listed by Reactor Building elevation and sampling location .....	92
49. Measured decontamination factors for loose and fixed I-129 surface activity listed by Reactor Building elevation and sampling location .....	93
50. Measured decontamination factors for total Cs-137 surface activity listed by Reactor Building elevation and sampling location .....	94
51. Measured decontamination factors for total Sr-90 surface activity listed by Reactor Building elevation and sampling location .....	95

52. Measured decontamination factors for total I-129 surface activity listed by Reactor Building elevation and sampling location .....	96
53. Mean decontamination factors for several nuclides listed by type of surface and elevation .....	97
54. Decontamination factors calculated using pre- and post-decontamination beta and gamma exposure rates data .....	98
55. Reactor Building surface Areas .....	100
56. Total surface activities in curies on Reactor Building surfaces .....	101
57. Percent of TMI-2 fission product core inventory measured on Reactor Building surfaces .....	102
58. Coefficients of power function fits of Cs-137 surface concentrations ( $\mu\text{Ci}/\text{cm}^2$ ) and beta (mrad/h) or gamma (mR/h) exposure rates .....	103

## INTRODUCTION

To measure the effectiveness of the gross decontamination experiment (principally a water spray technique) performed in the Three Mile Island Unit 2 (TMI-2) Reactor Building, the Technical Information and Examination Program's radiation and environment personnel made surface activity measurements before and after the experiment. Eighty-five surface samples were collected during Entries 25 and 26 (December 15 and 16, 1981) and an additional 95 surface samples were obtained during entries 54 and 55 (March 25 and 26, 1982). Radiological survey, thermoluminescent dosimetry, and gamma spectroscopy measurements were performed in conjunction with surface sampling to determine the correlation between surface contamination and radiation fields.

The surface samples were analyzed at the Idaho National Engineering Laboratory (INEL) using gamma spectroscopy, gross beta, and neutron activation analysis (NAA) techniques. These methods determined the surface concentrations of the gamma-emitting nuclides,  $^{137}\text{Cs}$ ,  $^{134}\text{Cs}$ ,  $^{125}\text{Sb}$ , and  $^{60}\text{Co}$ , the beta-emitting nuclide,  $^{90}\text{Sr}$ , and the x-ray emitter,  $^{129}\text{I}$ . The concentration of total fissile material (i.e.  $^{235}\text{U}$ ) was also determined for selected samples using a delayed fission neutron counting technique.

This report presents the results of these analyses as pre- and post-decontamination surface concentrations. Also presented are the beta and gamma exposure rates data that were collected concurrently with surface sampling using a gross beta/gamma survey instrument. In addition, decontamination factors (DFs) on a nuclide by nuclide basis are given for each location sampled.

## SAMPLING EQUIPMENT

### Surface Sampler

contamination within the TMI-2 Reactor Building relied primarily on the use of smears and radiological survey instruments. However, both of these methods were of limited use. Smears are of unquestioned value when used to determine the presence or absence of loose contamination, but are inadequate to quantify contamination especially if part of it is fixed. The survey instruments that were used lacked sufficient shielding to provide good collimation and, in addition, could not distinguish between gamma rays that originated from the surface of interest and those that passed through the surface having originated from other sources. This latter failing was particularly troublesome when survey measurements were made on the 305-ft elevation because of the contribution to the gamma flux from the highly contaminated water present in the Reactor Building basement. These shortcomings were serious enough to warrant development of a surface sampling device.

The surface sampler used to collect samples from horizontal surfaces at TMI-2 is shown in Figure 1. A similar tool having a smaller base plate was used to obtain samples from vertical surfaces. The sampler is a milling tool that has four major components: (a) a 1.27-cm diameter, 575 rpm, constant speed drill, (b) a drill support assembly that allows setting the sample collection depth, (c) filters for intake air purification and sample collection, and (d) an air pump that forces air across the surface being sampled and through the sample collection filter.

The drill support assembly serves several functions. It maintains a bit axis that is perpendicular to the plane of the base plate; it provides a positive stop for drill movement in the downward direction (the stop is the top surface of the cylindrical drill shaft extension receptacle), and it provides ports for connecting purification and sample filters. The disk-type flange that is welded at a height slightly below the top of the receptacle is marked in 22-1/2 degree intervals providing 16 numbered referenced marks.

Zero penetration depth is set while the base plate of the sampler is pressed firmly against the surface to be sampled. The depth setting disk is turned counterclockwise enough to have a separation between the setting disk and its stop while a slight downward pressure (towards the base plate) is applied on the drill. The setting disk turns freely when not in contact with the stop. While the milling bit is resting on the surface to be sampled, the reference zero is set by turning the depth setting disk clockwise until it just begins to bind against the stop. The reference zero is now read as the number that occupies the sector below the shaft of the disk locking 'T' handle.

Sampling depth may be set (after first zeroing the sampler) by turning the penetration depth setting disk counterclockwise the desired number of revolutions. Counterclockwise rotation of the disk from a zero setting will allow the bit to travel beyond the plane of the sampler's base plate when the drill is operated. Each counter revolution of the disk from a reference zero adds 0.635 mm to the penetration depth that will be achieved.

Figure 2 shows the oval sample vacuum chamber that is located on the bottom surface of the sampler's base plate. The chamber, which has an area of  $39.03 \text{ cm}^2$  and is 1.575-mm tall, is surrounded by a foam rubber gasket that when compressed seals the chamber. Air is drawn into the chamber through the circular port on the left and exits through the port located at the extreme right end of the chamber. The bit receptacle is centered at the larger end of the chamber near the sloping exhaust port. A bit is fastened to the drill shaft by inserting the threaded end of the bit into the bit receptacle and turning the bit clockwise until snug.

A detailed sketch of the sample filter cartridge is shown in Figure 3. The cartridge body is composed of plastic pipe fittings. The sample collection filter, a Whatman 16  $\mu\text{m}$  paper filter, is held in place in the coupler by two snap rings, a screen, and an 'o'-ring.

The cartridge is installed by removing the nylon tube cap and inserting the plastic intake tube into the exhaust port shown on the right of the cylinder that is the receptacle for the drill shaft extension (see Figure 1).

The stop for the tube is very near the point where the exhaust port enters the oval vacuum chamber so that cross-contamination between samples is minimized. The nylon tube plug is then removed and the coupler on the right in Figure 3 is inserted into the tygon tubing that is the header of the air pump.

### Calibration

The vertical and horizontal surface samplers that were used during December 1981 and March 1982 to collect samples at TMI-2 were received at the INEL during May 1982. After decontamination, they were both re-fitted with new drills, 'o'-rings, gaskets, non-skid pads, air purification filters, tygon tubing, and air pumps. The samplers were subsequently used to collect samples from standardized concrete and metal surfaces.

Four standardized surfaces were prepared, two of concrete and two of metal. The concrete slabs, which were each 35.6-cm square and 8.9-cm thick, were poured during March 1982. Each was faced so that no aggregate was visible and the surface was smooth and unpitted. After about three months of curing, each was brush painted with Keeler and Long No. 7107 Epoxy White Primer. They were allowed to dry for two days and then three adhesive strips, each 1.91-cm wide by about 6-cm long, were taped to each surface at locations on the diagonal. The slabs were then brush painted with a Keeler and Long E-1-7938 Epoxy Ivory Cream Enamel that had  $^{137}\text{Cs}$  added to produce a surface concentration of approximately  $0.1 \mu\text{Ci}/\text{cm}^2$ . A similar procedure was used to prepare the two metal surfaces except that the primer and finish paints used were Carbo Zinc II and Phenoline 368 WG, respectively, both manufactured by Carboline Co. The paints used are the same as those that were used to paint the corresponding types of surfaces within the TMI-2 Reactor Building.<sup>1</sup>

The surfaces were allowed to dry several days and then the adhesive strips were removed, cut to 2.54-cm lengths, and analyzed at the Radiation Measurements Laboratory (RML) using gamma spectrometry with lithium-drifted germanium [Ge(Li)] detectors to determine the absolute  $^{137}\text{Cs}$  surface concentrations.

Following the same sample collection procedure that was used at TMI-2, 15 samples were collected from one of the concrete blocks and four samples were collected from each of the other three standardized surfaces. The mean values of the  $^{137}\text{Cs}$  surface concentrations on the four standardized surfaces that were determined by analyzing milled samples and adhesive strips are given in Table 1 for comparison. Although the horizontal concrete surface was sampled to depths of 0.25, 1.27, and 3.18 mm, only one value for the surface activity on the horizontal concrete surface is given in Table 1 under "Milled Samples." The surface activity data indicate that the activity retention efficiency of the horizontal surface sampler is essentially independent of sampling depth for the three depths used. The variability in sample mass among samples that were intended to be collected to the same depth was more pronounced in samples collected from the TMI-2 Reactor Building than in the samples collected from the standardized surface. Unfortunately, only the masses of the samples collected during March 1982 were measured but it is reasonable to assume that the designated and actual sampling depths for samples collected during December 1981 were often not the same. Therefore, for the purpose of calculating the sampler's activity collection efficiency the results for all 15 milled horizontal concrete samples were averaged.

The mean surface activities in Table 1 for the vertical concrete and horizontal steel surfaces were each calculated using the analysis results for four milled samples. One milled vertical steel sample was rejected when calculating the mean surface activity on that surface because the penetration achieved was inadequate and paint remained. The surface activities given in Table 1 that were determined by analyzing adhesive strips are, in each case, the mean value measured on three strips. In each case the uncertainty given is one standard deviation of the mean.

The activity collection efficiencies of the horizontal and vertical surface samplers were calculated using the mean  $^{137}\text{Cs}$  surface concentrations given in Table 1. Activity collection efficiency for each type of surface is defined here as the ratio of the mean value of  $^{137}\text{Cs}$  concentration that was determined by analyzing milled samples to the mean value that

was determined by analyzing the corresponding adhesive strips. The efficiencies were found to be greater than one for all four surfaces. This implies that the actual surface areas removed by milling were larger than the cross sectional area of the bit, which was  $1.27 \text{ cm}^2$ . The efficiencies range from 1.1 for sampling done on vertical steel to 2.6 for sampling done on vertical concrete. The efficiency for vertical concrete surfaces is substantially higher than that for vertical steel surfaces probably because of the greater vibration induced when milling vertical concrete. The sampling efficiencies for horizontal steel and concrete surfaces are about the same, being 1.6 and 1.4, respectively. In each case, the uncertainty in the value for the efficiency was calculated at the one-sigma level by propagating the errors associated with the corresponding mean surface concentrations. The uncertainties in the efficiencies range from  $\pm 14\%$  for sampling done on horizontal concrete to  $\pm 27\%$  for sampling done on vertical steel. The efficiencies given in Table 1 were used to correct the surface activity concentrations on TMI-2 Reactor Building surfaces that were reported in EG&G Idaho internal technical reports.

#### Gross Beta/Gamma Survey Instrument

At each sampling location, measurements were made of the gross beta and gamma radiation fields prior to the collection of surface samples. The survey instruments used were all Eberline Instrument Corp. R0-2A's. The R0-2A is equipped with a Juno-type ionization chamber and a 0.0508-mm mylar window.<sup>2</sup> A slide on the bottom of the instrument can be moved to cover the window so as to allow measurement of the gamma component of a radiation field. A measurement made with the slide in the open-window provides a measure of the beta-plus-gamma field. Eberline states the accuracy of this instrument is  $\pm 5\%$  full scale and that its photon response is  $\pm 15\%$  from 12 keV to 1.3 MeV.<sup>2</sup>

To minimize contamination of the instruments each was bagged in plastic prior to use in the Reactor Building. Each instrument was similarly bagged in plastic during its calibration. A bracket having four pointed corner posts was attached to each survey instrument prior to use to provide a

constant source-detector geometry. The height of the corner posts was such as to provide a distance of one inch between the bottom surface of the instrument and the surface being measured.

## SAMPLING PROCEDURE

The procedure that was followed during surface sample collection required that a gross beta-gamma survey be made of the surface to be sampled prior to sample collection. At each location, both open- and closed-window measurements were made while the corner posts of the bracket previously described were in contact with the surface.

To minimize cross-contamination between samples, a new milling bit was installed in the surface sampler prior to collecting each sample. A carbide bit was used for milling concrete and cinder block surfaces, and a hardened steel bit was used for milling metal surfaces. The sample collection procedure used for horizontal surfaces included an initial vacuum of the surface without drill operation to remove loose particulates. Following the vacuum and prior to surface milling, a new sample filter cartridge was installed while the sampler remained stationary. The sample collection procedure used for both horizontal and vertical surfaces is given in detail in Appendix A.

The types of surfaces sampled and the number of locations sampled at each elevation are listed in Table 2. These locations are indicated in Figures 4 and 5 as numbered circles and triangles. Figure 4 is the floor plan for the entry-level floor at the 305-ft elevation and Figure 5 is the floor plan for the fuel handling floor at the 347-ft, 6-in. elevation. The circles correspond to sampling locations on horizontal surfaces and the triangles indicate locations where samples were collected from vertical surfaces. Sample locations 26 and H1 (see Figure 5) are both on the 'A' D-ring walkway at the 367-ft, 4-in. elevation and locations I and 22 are on the southern I beam that supports reactor coolant pump 2A. Not shown in Figure 5 is sample location H8 on the elevator shaft roof because the location was eliminated when samples were collected during March 1982.

The sampling procedure stipulated that samples were to be collected to a depth of 1.27 mm from all vertical and horizontal metal surfaces, and the standard sampling depth was to be 3.18 mm for all horizontal concrete surfaces. In an attempt to determine whether activity had migrated into painted concrete, samples were collected from floors at multiple depths at

each of six sampling locations before decontamination operations began and at seven locations following completion of decontamination. Sampling was intended to be done at depths from 0.25 to 3.18 mm in the same vicinity at each of these floor locations.

In order to estimate the actual sampling depths achieved during surface sampling, the net masses of the millings of the March 1982 surface samples were measured. For each milled sample, its net mass was calculated by subtracting the measured mean mass of the 38 vacuum samples collected in March, which was  $0.23 \pm 0.03$  g, from the mass of its filter plus collected millings. The calculated net masses for these post-decontamination samples are given in Table 3 listed by type of surface. Negative net masses are reported as zeroes in the table. These masses may be compared with the theoretical masses corresponding to sampling depths of 0.25, 1.27, and 3.18 mm. If we assume that the sample core radius is a constant 6.35 mm (the radius of the milling bit) and that for concrete surfaces the sample density is  $2 \text{ mg/mm}^3$ , then these depths in concrete correspond to sample masses of 0.06, 0.32, and 0.80 g, respectively. The first assumption is based on the observation that milling of horizontal concrete usually removed an area of paint that was larger than the cross sectional area of the sample hole. The mean measured masses of the millings of concrete samples that were intended to be collected to depths of 0.25, 1.27, and 3.18 mm are, respectively,  $0.26 \pm 0.15$ ,  $0.24 \pm 0.19$ , and  $0.71 \pm 0.35$  g. It is apparent that on the average, the 0.25 mm samples were actually collected to a depth about the same as that of the 1.27 mm samples.

The masses of the horizontal concrete samples reported in Table 3 were converted to sampling depths after making the same assumptions previously used. The calculated depths for sampling the 0.25, 1.27, and 3.18 mm concrete samples are given in Table 4. The mean values of the calculated sampling depths corresponding to these intended sampling depths are  $1.00 \pm 0.60$ ,  $0.93 \pm 0.75$ , and  $2.75 \pm 1.36$  mm, respectively. Therefore, on the average, samples were collected at only two depths at floor locations where multiple samples were collected.

Keeler and Long, Inc. provided the paints that were applied on unlined concrete surfaces within the TMI-2 Reactor Building. They report<sup>3</sup> the dry film thicknesses of No. 6548 epoxy block filler, No. 7107 epoxy white primer, and No. 7475 epoxy white enamel finish paint as 0.142, 0.076, and 0.064 mm, respectively. The sum of these is 0.282 mm, a value substantially smaller than the calculated depths of sampling for all but three floor samples collected during March 1982. All of the March samples were visually examined following downloading of the sample filter cartridges into petri dishes, and these three samples, 34F2, 54F4 (1), and 54F4 (2) were found to contain a small amount of concrete dust in addition to paint shavings. The negligible sampling depths calculated for these three samples are probably due to larger than normal filter diameters.

## ANALYSIS METHODS

The samples arrived at the INEL as filter cartridges containing concrete and paint shavings, metal and paint shavings, paint shavings only, or in the case of vacuum samples, just a few dozen small particles. To achieve a sample configuration compatible with existing RML gamma analysis geometries, the sample filter cartridges were downloaded and each sample was transferred to a 150-mL polyethylene bottle. The collected millings and filters in the sample cartridges were initially transferred to separate, pre-weighed petri dishes. After first removing the milling bit, each cartridge was opened with the exhaust side oriented down and then in turn each half of the cartridge was held over the petri dish and tapped with a small hand tool. The filter was then removed and placed in the same petri dish. The snap and 'o'-rings were replaced in the cartridge half that held the filter and the cartridge was reassembled.

The cartridge's internals were then washed with 50 mL 1N HCl spiked with 3.3 mg Na<sub>2</sub>SO<sub>3</sub> and 3.3 mg KI. After the solution was poured into the cartridge, the cartridge was shaken vigorously and the liquid was then decanted into a 150-mL polyethylene bottle. This procedure was repeated using 50 mL of deionized water. The milling bit was placed in a test tube, 5 mL of the same acidic solution was added, the test tube was shaken vigorously, and the liquid was decanted into the same polyethylene bottle. This was repeated using 5 mL of deionized water.

With each sample, a small amount of wash solution was poured from the sample bottle into the corresponding petri dish containing the millings and filter. Using tweezers, the filter was rolled into a cylinder and inserted into the sample bottle. The liquid in the petri dish was then decanted into the same bottle. The petri dish was washed again using about 5 mL of the same solution from the sample bottle. A spatula was used to remove any remaining particulates and they were transferred to the sample bottle. Thus, after the preparations described above, the 110 mL of liquid that had been used to wash the sample cartridge and milling bit, and the sample filter and collected millings were combined in a 150-mL polyethylene bottle.

Analysis techniques that were used on these samples included gamma spectroscopy, gross beta counting, NAA, and NAA/delayed fission neutron (DFN) counting. Each of the 180 surface samples was analyzed for gamma emitting nuclides; however, because of cost and time considerations not all samples were analyzed for  $^{90}\text{Sr}$ ,  $^{129}\text{I}$ , or fissile material. Ninety-two samples were analyzed for  $^{90}\text{Sr}$ , 44 were analyzed for  $^{129}\text{I}$ , and 37 were analyzed for fissile material. Certain samples were combined prior to analysis for  $^{90}\text{Sr}$ ,  $^{129}\text{I}$ , or  $^{235}\text{U}$ . The vacuum and milled samples collected at sampling location 34 were separately consolidated prior to analyzing for  $^{90}\text{Sr}$ . The same applies to samples collected at sampling locations H10 and 91 that were analyzed for  $^{129}\text{I}$ . The vacuum samples collected at sampling locations H7, 54, and 149 were separately combined prior to analysis for  $^{90}\text{Sr}$  and  $^{235}\text{U}$ .

Measured activities in  $\mu\text{Ci}/\text{sample}$  were converted to surface concentrations in  $\mu\text{Ci}/\text{cm}^2$  by two different methods depending on whether the sample was collected by vacuuming only or by milling. The results for milled samples were divided by the bit milling area,  $1.27 \text{ cm}^2$ , and by the sampler activity collection efficiency corresponding to the type of surface sampled to provide surface activities in  $\mu\text{Ci}/\text{cm}^2$ . The efficiencies used are those listed in Table 1. The results for vacuum samples in  $\mu\text{Ci}/\text{sample}$  were converted to surface activities in  $\mu\text{Ci}/\text{cm}^2$  by assuming (a) the surface vacuumed in each case had an area of  $39.03 \text{ cm}^2$ , which is the area enclosed by the sampler's vacuum chamber, (b) the activity collected during vacuuming without drill operation was evenly distributed over  $39.03 \text{ cm}^2$ , and (c) the activity collection efficiency of the sampler during vacuuming was 100%. These assumptions were necessary because the loose particulates activity collection efficiency of the sampler was not measured during sampler calibration. The total surface activity concentration was determined by summing for each sample set the milled and vacuum sample results in  $\mu\text{Ci}/\text{cm}^2$ . A detailed description of each analysis method that was used is given in Appendix B.

## RESULTS

The data tables that follow often present surface concentrations by sample (e.g. 70F1) or by sample location (e.g. 70). These two identification numbers are simply related; samples collected at a given location were all given sample numbers prefixed with the sample location number.

The surface activity concentration results for both the December 1981 and March 1982 samples are presented in  $\mu\text{Ci}/\text{cm}^2$  (decay-corrected to March 26, 1982) in Tables 5 through 29. Tables 5 through 16 present the results for each sample while Tables 17 through 29 give mean surface concentrations of the detected radionuclides by sampling location. The uncertainties in the concentrations determined by analysis of milled samples are given at the one sigma level and are due to counting statistics and the uncertainties in the activity collection efficiencies of the samplers. The uncertainties in the concentrations determined by analysis of vacuum samples are given at the one sigma level and are due to counting statistics only. Unfortunately, the analysis software of the gamma spectrometry system used for this work did not have as a feature automatic detection limit calculation. Therefore, less-than detectable concentrations of  $^{125}\text{Sb}$  and  $^{60}\text{Co}$  are simply footnoted in the tables.

Table 30 presents the December 1981 mean  $^{137}\text{Cs}$  surface concentration in  $\mu\text{Ci}/\text{cm}^2$  (decay-corrected to March 26, 1982) at each sampling location arranged by type of surface and elevation (i.e., 305 ft-0 in., etc.). Similar results for  $^{134}\text{Cs}$ ,  $^{90}\text{Sr}$ ,  $^{129}\text{I}$ , and  $^{125}\text{Sb}$  are given in Tables 31, 32, 33, and 34, respectively. Mean surface concentrations presented in these tables were calculated for horizontal and vertical concrete and horizontal and vertical metal at each of three sampling elevations. The uncertainties in the means are each the standard deviation of the mean calculated at the one sigma level. The mean December 1981 surface concentrations of these five radionuclides are compiled in Table 35. The mean values of the ratios of the December 1981 surface concentrations of several radionuclides to the concentration of  $^{137}\text{Cs}$  measured in each surface sample are given for both vacuum and milled samples in Table 36.

Table 37 presents the March 1982 mean  $^{137}\text{Cs}$  surface concentration in  $\mu\text{Ci}/\text{cm}^2$  (decay-corrected to March 26, 1982) at each sampling location arranged by type of surface and elevation. Similar results for  $^{134}\text{Cs}$ ,  $^{90}\text{Sr}$ ,  $^{129}\text{I}$ , and  $^{125}\text{Sb}$  are given in Tables 38, 39, 40, and 41, respectively. The mean March 1982 surface concentrations of these five radionuclides on horizontal and vertical concrete and metal surfaces are listed in Table 42 by sampling location elevation. Table 43 presents the mean values of the ratios of the March 1982 surface concentrations of five radionuclides to the concentration of  $^{137}\text{Cs}$  measured in each surface sample. The ratios for both vacuum and milled samples are given in this table.

Tables 44 and 45 present, respectively, the beta and gamma exposure rates that were measured during December 1981 and March 1982 using R02-A survey meters. Mean values of these exposure rates are listed in Table 46 arranged by type of surface and Reactor Building elevation. Beta exposure rates are given in mRad/h and gamma exposure rates are given in mR/h. These data were not decay-corrected.

DFs for  $^{137}\text{Cs}$ ,  $^{90}\text{Sr}$ , and  $^{129}\text{I}$  are given, respectively, in Tables 47, 48, and 49. The DFs for vacuum and milled samples are given separately for each location sampled. The DF for each nuclide was calculated as the ratio of the mean surface activity measured at a given sampling location before decontamination to the mean surface activity measured at the same location after decontamination. All activities were decay-corrected to March 26, 1982 prior to calculation of DFs. The data in these tables are arranged by type of surface and by Reactor Building elevation. Decontamination factors were also calculated using total surface activities, these totals being for each nuclide the sum of the mean loose particulate activity and the mean fixed activity measured at a given sampling location. Values of these DFs for  $^{137}\text{Cs}$ ,  $^{90}\text{Sr}$ , and  $^{129}\text{I}$  are presented by sampling location in Tables 50, 51, and 52 respectively. Mean DFs for several radionuclides are listed by type of surface and by Reactor Building elevation in Table 53. The results for both vacuum and milled samples are presented separately in this table. Table 54 presents the DFs by sampling location that were calculated using pre- and post-decontamination beta and gamma exposure rates. Mean exposure rate DFs for four generic surfaces are also given in this table.

## DISCUSSION

### Surface Activities

Prior to decontamination, floors on both Reactor Building elevations were considerably more contaminated than walls, as might be expected. The ratios of the average surface concentrations of  $^{137}\text{Cs}$  and  $^{90}\text{Sr}$  on the concrete floor to their corresponding average concentrations on the D-ring wall are, respectively 90 to 1 and 190 to 1 on the 305-ft elevation and 80 to 1 and 160 to 1 for the 347-ft elevation. The mean surface concentrations compiled in Table 35 indicate that the average concentrations of all nuclides except  $^{125}\text{Sb}$  were about the same on both floors. The concentration of this nuclide was about a factor of 10 higher on the 305-ft elevation floor than it was on the 347-ft elevation, and its concentration was less than detectable on the 'A' D-ring walkway, which is at an elevation of 367 ft. The mean December 1981 concentrations of  $^{137}\text{Cs}$  and  $^{90}\text{Sr}$  on the 305-ft elevation were, respectively,  $3.6 \pm 0.9$  and  $0.17 \pm 0.04 \mu\text{Ci}/\text{cm}^2$  and their concentrations on the 347-ft elevation floor were  $2.5 \pm 0.7$  and  $0.3 \pm 0.2 \mu\text{Ci}/\text{cm}^2$ , respectively.

The sampling location having the highest mean  $^{137}\text{Cs}$  surface activity before decontamination was floor location H7, which is beneath the northeast corner of core flood tank 'A'. The mean  $^{137}\text{Cs}$  activity at this location was  $8 \mu\text{Ci}/\text{cm}^2$  which is only about a factor of four higher than the lowest local mean  $^{137}\text{Cs}$  concentration measured on the 305-ft elevation. However, surface activities were found to vary by factors sometimes this large or larger over small areas of floor. Samples were collected in the same vicinity, usually from points not more than a few inches apart, at locations 50, 34, and H7 on the 305 ft elevation and at locations 54, H10, and 91 on the 347 ft elevation. Samples were collected at each of these locations to different depths in an attempt to determine if activity had migrated into the concrete. The surface activity of  $^{137}\text{Cs}$ , prior to decontamination, varied by factors of 2.2, ~1 and 12.9 for locations 50, 34, and H7; and 2.0, 3.8, and 3.2 for locations 54, H10, and 91. Following decontamination, surface activities varied by factors of 30, 2.1, 3.6, 6.4, 3.7, and 2.3,

respectively. This nonhomogeneity of surface activity over small areas nullifies any conclusions regarding activity penetration that might be drawn from these surface activity data.

Of the locations whose samples were analyzed for  $^{90}\text{Sr}$ , location 149 had the highest pre-decontamination surface activity. That value was  $1.0 \pm 0.1 \mu\text{Ci}/\text{cm}^2$ . The mean value of the ratio of  $^{90}\text{Sr}$  to  $^{137}\text{Cs}$  that was calculated for each sample collected from the 305-ft elevation is  $4 \pm 2 \text{ E-2}$ . Similar ratios for  $^{134}\text{Cs}$ ,  $^{125}\text{Sb}$ ,  $^{60}\text{Co}$ , and  $^{129}\text{I}$  for various types of Reactor Building surfaces were presented in Table 36. The  $^{90}\text{Sr}$  to  $^{137}\text{Cs}$  ratio for all vacuum samples collected from horizontal surfaces at all elevations is  $7 \pm 6 \text{ E-2}$  while that for all milled samples collected from the same surfaces is  $5 \pm 4 \text{ E-2}$ . The same ratio for all samples collected from vertical surfaces is  $4 \pm 1 \text{ E-2}$ . The values of these ratios are essentially equal to the value of the ratio of the concentrations of  $^{90}\text{Sr}$  to  $^{137}\text{Cs}$  that was measured in the liquid samples collected from the Reactor Building basement on May 14, 1981.<sup>4</sup> The value of this latter ratio,  $3.7 \text{ E-2}$ , was computed after decay correcting the concentrations in  $\mu\text{Ci}/\text{mL}$  to March 26, 1982, the date to which all of the surface concentrations in this report have been decay-corrected. This equality implies that the mode of transport of the  $^{90}\text{Sr}$  from the contaminated water in the basement to Reactor Building surfaces was in water droplets and that the majority of the  $^{90}\text{Sr}$  was transported to the walls and floors after it had reached chemical equilibrium in the basement water.

Sufficient surface activity data was collected before decontamination to make possible calculations of the fractions of the total core inventories of certain fission products that were deposited and which remained on Reactor Building surfaces. What is needed to perform these calculations is an itemized list of Reactor Building surface areas. That list is provided in Table 55. The surface areas of the four generic surfaces<sup>5</sup> (i.e. horizontal and vertical concrete and steel surfaces) are given in this table. The areas of these surfaces at three different elevation intervals were calculated so that mean surface concentrations on surfaces lying within these intervals could be used directly. Since no surface samples were collected from the Reactor Building basement during the December sample collection

period, the surface activities used for that region of the building were those measured on the 305-ft elevation. Similarly the concentrations used for surfaces at 347-ft, 6-in. elevation and above were estimated as the average of the mean December 1981 surface activities measured on the 347-ft, 6-in. and 367-ft, 4-in. elevations. Using the measured December surface concentrations and the surface areas from Table 55, the total activities of  $^{137}\text{Cs}$ ,  $^{90}\text{Sr}$ ,  $^{129}\text{I}$ , and  $^{125}\text{Sb}$  on various Reactor Building surfaces were calculated. Those activities (measured in curies) are presented in Table 56.

Total core inventories of these nuclides and their calculated inventories on Reactor Building surfaces are given in Table 57. The total core inventories listed are those that were calculated using the ORIGEN-2 Code<sup>6</sup> and have been decay-corrected to March 26, 1982. It is evident that the percentages of the core inventories of these nuclides deposited on Reactor Building surfaces are all very small (see Table 58). Excluding iodine, the values range from  $2.4 \times 10^{-3}$  for  $^{90}\text{Sr}$  to  $4.7 \times 10^{-2}$  for  $^{134}\text{Cs}$ . This latter value is 34% higher than its true value if we assume the  $^{137}\text{Cs}$  core inventory to be correct, since the percentage of  $^{137}\text{Cs}$  deposited on surfaces is  $3.5 \times 10^{-2}$ . The highest percentage of the five nuclides listed is that of  $^{129}\text{I}$  and the value for it is  $5.7 \times 10^{-2}$ . The core inventory of  $^{131}\text{I}$  at the time of shutdown was  $7.0 \times 10^7 \text{ Ci}$ . If we assume that the same fraction of  $^{129}\text{I}$  was on the floors and walls of the Reactor Building shortly after reactor scram we can readily estimate the initial surface concentration of  $^{131}\text{I}$  on those surfaces. Multiplying the  $^{131}\text{I}$  inventory by the deposition fraction for  $^{129}\text{I}$  and dividing this result by  $2.20 \times 10^8 \text{ cm}^2$ , the total internal Reactor Building surface area, one arrives at a March 28, 1979 average  $^{131}\text{I}$  surface concentration of  $180 \mu\text{Ci}/\text{cm}^2$ .

Several sets of surface samples were collected during December 1981 from an area of the 305-ft elevation just south of the open stairwell. Samples collected at one of the locations in this area, location 55, which is near the containment wall, were found to contain  $^{144}\text{Ce}$ . Because Ce is usually associated with fuel, these samples were subjected to analyses for fissile material. The vacuum and milled samples identified as 55F1 and 55F2, respectively, did contain detectable amounts of  $^{235}\text{U}$ . The surface